Biochemical Pharmacology 130 (2017) 34–50

Contents lists available at ScienceDirect

Biochemical Pharmacology

journal homepage: www.elsevier.com/locate/biochempharm

Novel human bioactive peptides identified in Apolipoprotein B: Evaluation of their therapeutic potential

Rosa Gaglione [a,b], Eliana Dell'Olmo [a], Andrea Bosso [b,c], Marco Chino [a], Katia Pane [c], Flora Ascione [d], Francesco Itri [a], Sergio Caserta [d,e,f], Angela Amoresano [a], Angelina Lombardi [a], Henk P. Haagsman [b], Renata Piccoli [a,g], Elio Pizzo [c], Edwin J.A. Veldhuizen [b], Eugenio Notomista [c], Angela Arciello [a,g,*]

[a] Department of Chemical Sciences, University of Naples Federico II, 80126 Naples, Italy
[b] Department of Infectious Diseases and Immunology, Division Molecular Host Defence, Faculty of Veterinary Medicine, Utrecht University, Utrecht, The Netherlands
[c] Department of Biology, University of Naples Federico II, 80126 Naples, Italy
[d] Department of Chemical, Materials and Production Engineering, University of Naples Federico II, 80125 Naples, Italy
[e] CEINGE Biotecnologie Avanzate, Via Sergio Pansini, 5, 80131 Naples, Italy
[f] Consorzio Interuniversitario Nazionale per la Scienza e Tecnologia dei Materiali (INSTM), UdR INSTM Napoli Federico II, P.le Tecchio, 80, 80125 Naples, Italy
[g] Istituto Nazionale di Biostrutture e Biosistemi (INBB), Italy

ARTICLE INFO

Article history:
Received 2 December 2016
Accepted 23 January 2017
Available online 25 January 2017

Keywords:
Host defence peptides
Apolipoprotein B
Immunomodulation
Lipopolysaccharide
Bacterial biofilm
Combination therapy
Wound healing
Biocompatibility

ABSTRACT

Host defence peptides (HDPs) are short, cationic amphipathic peptides that play a key role in the response to infection and inflammation in all complex life forms. It is increasingly emerging that HDPs generally have a modest direct activity against a broad range of microorganisms, and that their anti-infective properties are mainly due to their ability to modulate the immune response. Here, we report the recombinant production and characterization of two novel HDPs identified in human Apolipoprotein B (residues 887–922) by using a bioinformatics method recently developed by our group. We focused our attention on two variants of the identified HDP, here named r(P)ApoB$_L$ and r(P)ApoB$_S$, 38- and 26-residue long, respectively. Both HDPs were found to be endowed with a broad-spectrum antimicrobial activity while they show neither toxic nor haemolytic effects towards eukaryotic cells. Interestingly, both HDPs were found to display a significant anti-biofilm activity, and to act in synergy with either commonly used antibiotics or EDTA. The latter was selected for its ability to affect bacterial outer membrane permeability, and to sensitize bacteria to several antibiotics. Circular dichroism analyses showed that SDS, TFE, and LPS significantly alter r(P)ApoB$_L$ conformation, whereas slighter or no significant effects were detected in the case of r(P)ApoB$_S$ peptide. Interestingly, both ApoB derived peptides were found to elicit anti-inflammatory effects, being able to mitigate the production of pro-inflammatory interleukin-6 and nitric oxide in LPS induced murine macrophages. It should also be emphasized that r(P)ApoB$_L$ peptide was found to play a role in human keratinocytes wound closure *in vitro*. Altogether, these findings open interesting perspectives on the therapeutic use of the herein identified HDPs.

1. Introduction

The excessive and sometimes improper use of antibiotics has been responsible for the development of resistant bacterial isolates, the so-called 'superbugs', such as methicillin-resistant *Staphylococcus aureus* (MRSA) [1], vancomycin-resistant enterococci (VRE), and multidrug-resistant *Pseudomonas*, *Klebsiella*, and *Acinetobacter* [2]. This made the search for novel antimicrobial therapies and approaches imperative. In this scenario, the broad immunomodulatory properties of naturally occurring host defence peptides (HDPs) have attracted considerable attention. HDPs, also known as antimicrobial peptides (AMPs), are evolutionarily conserved molecules of the innate immune system. They are a

Abbreviations: MRSA, methicillin-resistant *Staphylococcus aureus*; VRE, vancomycin-resistant enterococci; HDPs, host defence peptides; AMPs, antimicrobial peptides; LPS, lipopolysaccharide; ApoE, Apolipoprotein E; ApoB, Apolipoprotein B; LDL, low-density lipoprotein; IL-10, interleukin-10; MIC, minimal inhibitory concentration; TSA, Tryptic Soy Agar; AS, absolute score; MHB, Muller Hinton Broth; NB, Nutrient Broth; IPTG, isopropyl-β-D-thiogalactopyranoside; TFE, trifluoroethanol; SDS, sodium dodecyl sulfate; FIC, fractional inhibitory concentration; EDTA, ethylenediaminetetraacetic acid; IL-6, interleukin-6; NO, nitric oxide; CATH-2, cathelicidin-2; ONC, onconase; PBS, phosphate-buffered saline; CD, circular dichroism; MTT, 3-(4,5-dimethylthiazol-2-yl)-2,5-diphenyltetrazolium bromide; MALDI-MS, matrix assisted laser desorption ionisation mass spectrometry; RBCs, red blood cells; WH, wound healing.

* Corresponding author at: Department of Chemical Sciences, University of Naples Federico II, 80126 Naples, Italy
E-mail address: anarciel@unina.it (A. Arciello).

http://dx.doi.org/10.1016/j.bcp.2017.01.009
0006-2952/

key element of the ancient, nonspecific innate defence system in most multicellular organisms, representing the first line of defence against invading microbes [3,4]. Found in all complex living organisms, HDPs have first attracted considerable attention for their modest antimicrobial activity directed towards a broad spectrum of pathogens including bacteria, viruses, fungi, and protozoa [3,4]. Natural HDPs have a size ranging from 12 to 50 amino acids, are mostly cationic owing to the presence of high levels of lysine and arginine residues, and contain over 50% hydrophobic amino acids [3,5]. These properties are at the basis of HDPs' ability to interact with membranes, and, in some cases, to penetrate cell membranes. In model systems, HDPs associate preferentially with negatively charged membranes of bacteria-like composition, but many peptides are also able to translocate into host cells. To date, the molecular bases of their selectivity towards bacterial membranes are still poorly understood [6]. It has been suggested that HDPs tend to translocate into bacterial cells owing to the presence of a large electrical potential gradient [7]. However, although HDPs' direct antimicrobial mechanism of action against bacteria mainly involves interaction with the bacterial membrane, multiple targets have been identified, such as cell wall peptidoglycans, cytosolic RNA, proteins, or cytosolic enzymes/chaperones [6,8]. Hence, the selection of resistance mechanisms in bacteria is improbable, since the removal of a single target, *e.g.* by mutation, would still allow other targets to mediate HDPs direct killing activity [8]. However, it is becoming increasingly evident that these peptides are endowed with a wide range of biological activities, such as multispecies anti-biofilm properties, modulation of innate immune response, and anticancer, analgesic, antioxidant and anti-inflammatory activities [3,9–13]. Therefore, although these bioactive peptides were often named AMPs, more recently they have been termed as HDPs to describe more appropriately the breadth of their activities [14]. Due to HDPs' multifunctional properties, as well as to the increased bacterial resistance to conventional antibiotics, these peptides have great chance to be used as anti-infective and immunomodulatory therapeutics. Although very few HDPs are currently in use in the market, many of them are progressing through clinical trials for the treatment of diseases including microbial infections, organ failure, immune disorders, wound healing, diabetes and cancer [15,16]. Currently, most of the therapies based on HDPs that have entered clinical trials were designed for topical applications [17], presumably due to issues concerning their stability and toxicity [18].

Natural cationic HDPs are encoded by genes from many organisms. In mammals, HDPs are expressed in a variety of cell types including monocytes/macrophages, neutrophils, epithelial cells, keratinocytes, and mast cells [19–21]. They are usually synthesized as pro-peptides from which mature and biologically active HDPs are released by bacterial and/or host proteases [20]. Apolipoproteins are a source of bioactive peptides. Previous reports have shown that peptides derived from the cationic receptor binding region of Apolipoprotein E (ApoE141-149) are endowed with broad anti-infective activity [22]. Apolipoprotein B (ApoB) also contains two LDL (low-density lipoprotein) receptor binding domains, namely region A (ApoB3147-3157) and region B (ApoB3359-3367). Region B, more uniformly conserved across species and primarily involved in receptor binding, has been found to be endowed with a significant antiviral activity [22]. Moreover, peptides derived from ApoB have been already used in vaccine preparations to treat atherosclerosis [23]. When ApoE deficient mice have been immunized with ApoB661–680 and ApoB3136–3155 peptides, a significant increase of the levels of peptide-specific immunoglobulins was detected accompanied by a concomitant increase of secreted interleukin-10 (IL-10) levels, with no effect on IFN-γ expression levels, thus indicating that ApoB derived peptides are able to modulate the immune response [23].

Recently, our group developed an *in silico* method [K. Pane et al. submitted, 24] to identify HDPs in protein precursors and to predict quantitatively their antibacterial activity. This method assigns to any given peptide an antimicrobial score, called "absolute score" (AS), on the basis of net charge, hydrophobicity and length of the peptide and of two bacterial strain-dependent weight factors defining the contribution of charge and hydrophobicity to the antimicrobial activity. We demonstrated that AS is directly proportional to the antimicrobial activity of HDPs expressed as Log(1000/MIC), where MIC is the minimal inhibitory concentration of the peptide. Score values lower than 6.5 are considered not significant as they correspond to predicted MIC values higher than 200 μM, while for score values higher than about 10 the linear relationship is no longer valid, and an increase in the score does not necessarily correspond to a concomitant increase in the antimicrobial activity. In order to analyse a protein potentially bearing hidden antimicrobial regions, the AS values of all the peptides of the desired length contained in a precursor protein can be plotted as a function of peptide sequence and length, thus obtaining an accurate map of the antimicrobial activity determinants. This method allows the identification of novel HDPs within the sequence of known proteins ("cryptic" HDPs), as demonstrated by the identification of a novel cationic HDP endowed with antibacterial and immunomodulatory activities in human ApoE [24], and in the transcription factor Stf76 from the archaeon *Sulfolobus islandicus*. In the last case, peptide VVL-28 represents the first antimicrobial peptide derived from an archaeal protein [25].

On the basis of the interesting results obtained in the case of human ApoE, we applied our *in silico* analysis method to a human Apolipoprotein B (ApoB) isoform [26,27]. In Fig. 1, the isometric plot of region 882–929 of this ApoB variant is shown. An absolute maximum, corresponding to region 887–922 (AS = 12.0), and a relative maximum, corresponding to residues 887–909 (AS = 10.6), are shown (Fig. 1). Even if several ApoB functional regions have already been analysed, and in some cases biologically active peptides were obtained [22,23], to the best of our knowledge, this is the first report identifying ApoB region 887–922 as a source of HDPs.

Here, we report the recombinant production and characterization of two variants of the putative HDP identified by our bioinformatics method in human ApoB, *i.e.* peptides ApoB887-923 and ApoB887-911. Both peptides include at the C-terminal side one (as in the case of ApoB887-923), or two (as in the case of ApoB887-911) small uncharged residues (serine, glycine or threonine), which are not present in the regions highlighted in the AS plot (Fig. 1). These residues have been arbitrarily included to avoid that the negatively charged C-terminus of the peptide is adjacent to the antimicrobial region.

To evaluate the therapeutic potential of these peptides, we analysed their structure, antimicrobial and anti-biofilm activities, the ability to act in synergy with conventional antibiotics, their anti-inflammatory and wound healing properties, and their possible toxic effects on eukaryotic cells.

2. Materials and methods

2.1. Bacterial strains and growth conditions

Eight bacterial strains were used in the present study, *i.e. E. coli* ATCC 25922, methicillin-resistant *Staphylococcus aureus* (MRSA WKZ-2), *Salmonella enteriditis* 706 RIVM, *Bacillus globigii* TNO BM013, *Bacillus licheniformis* ATTC 21424, *Staphylococcus aureus* ATTC 29213, *Pseudomonas aeruginosa* ATCC 27853, and *Pseudomonas aeruginosa* PAO1. All bacterial strains were grown in Muller Hinton Broth (MHB, Becton Dickinson Difco, Franklin Lakes, NJ)

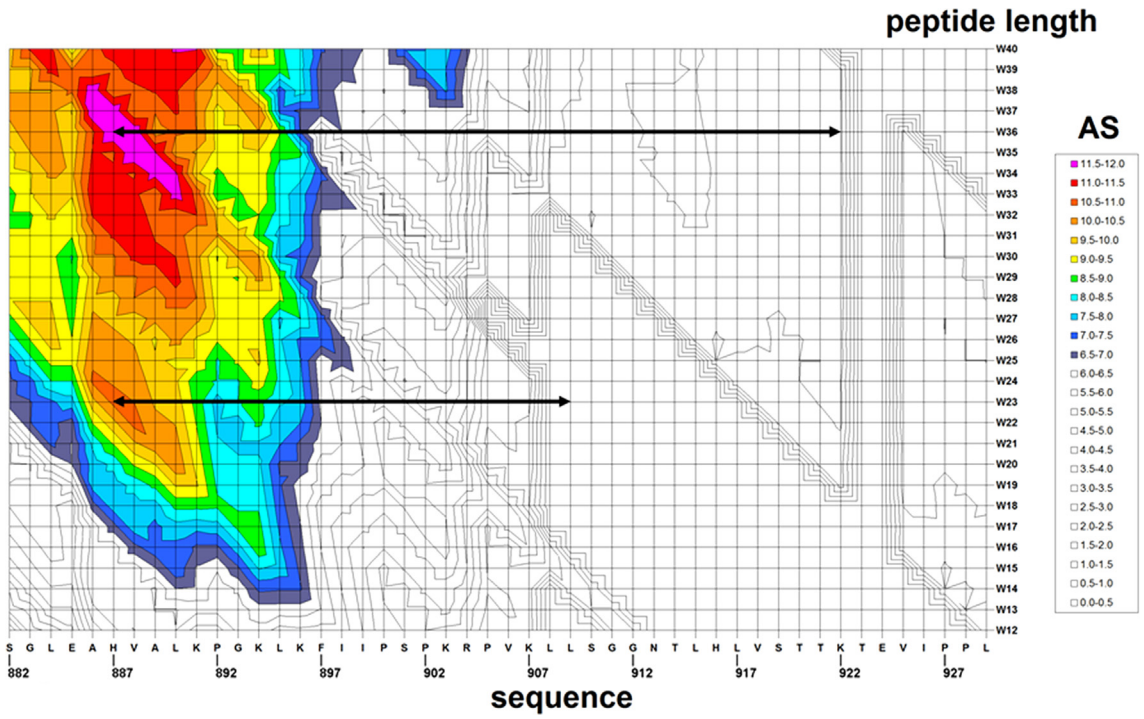

Fig. 1. Isometric plot showing the absolute score values (AS) of peptides with a length ranging from 12 to 40 residues (W12-W40) in the region 882–929 of ApoB. Colors were used to highlight AS values higher than 6.5, and corresponding to predicted MIC values on *S. aureus* lower than 200 μM.

and on Tryptic Soy Agar (TSA; Oxoid Ltd., Hampshire, UK). In all the experiments, bacteria were inoculated and grown overnight in MHB at 37 °C. The next day, bacteria were transferred to a fresh MHB tube and grown to mid-logarithmic phase.

2.2. Cell culture

Murine RAW 264.7 cells, malignant SVT2 murine fibroblasts (BALBc 3T3 cells transformed by SV40 virus), parental murine BALBc 3T3 cells, and human HeLa and HaCaT cells were from ATCC, Manassas, VA. Cells were cultured in Dulbecco's modified Eagle's medium (Sigma Aldrich, Milan, Italy), supplemented with 10% foetal bovine serum (HyClone, GE Healthcare Lifescience, Chicago, IL) and antibiotics, in a 5% CO_2 humidified atmosphere at 37 °C.

2.3. Synthetic peptides

CATH-2 peptide was obtained from CPC Scientific Inc. (Sunnyvale, USA), and LL-37 peptide was from Sigma Aldrich, Milan, Italy.

2.4. Expression ad isolation of recombinant ApoB derived peptides

Expression and isolation of recombinant peptides was carried out as previously described [24,28]. Briefly, *E. coli* BL21(DE3) cells were transformed with pET recombinant plasmids, and grown in 10 mL of Terrific Broth medium (TB) containing 100 μg/mL of ampicillin, at 37 °C up to OD_{600nm} of 2. These cultures were used to inoculate 1 L of TB/ampicillin medium. Glucose at final concentration of 4 g/L was added to cultures to limit protein expression before induction with IPTG. Cultures were incubated at 37 °C up to OD_{600nm} of 3.5–4. Expression of recombinant proteins was induced by addition of IPTG (isopropyl-β-D-thiogalactopyranoside) at final concentration of 0.7 mM. Cells were harvested after overnight induction by centrifugation at 8,000*g* for 15 min at 4 °C and washed with 50 mM Tris–HCl buffer pH 7.4. The bacterial pellet was suspended in 50 mM Tris-HCl buffer pH 7.4 containing 10 mM ethylenediaminetetraacetic acid (EDTA), and sonicated in a cell disruptor (10 x 1 min cycle, on ice). The suspension was then centrifuged at 18,000*g* for 60 min at 4 °C. The insoluble fractions were washed three times in 0.1 M Tris–HCl buffer pH 7.4 containing 10 mM EDTA, 2% Triton X-100, and 2 M urea, followed by repeated washes in 0.1 M Tris–HCl buffer pH 7.4. Following washing steps, 100 mg of fusion proteins were dissolved in 10 mL of denaturing buffer (6 M guanidine/HCl in 50 mM Tris–HCl, pH 7.4) containing 10 mM β-mercaptoethanol. Mixtures were incubated at 37 °C for 3 h under nitrogen atmosphere on a rotary shaker, and then centrifuged at 18,000*g* for 60 min at 4 °C. Soluble fractions were then collected and purified by affinity chromatography on Ni Sepharose™ 6 Fast Flow resin (GE Healthcare Lifescience, Chicago, IL). The chromatographic fractions were analysed by 15% SDS/PAGE, pooled, and extensively dialyzed against 0.1 M acetic acid pH 3 at 4 °C. Any insoluble material was removed by centrifugation and filtration. The sample containing the fusion construct was then acidified to pH 2.0 by the addition of 0.6 M HCl to allow the cleavage of Asp-Pro linker peptide, purged with N_2, and incubated at 60 °C for 24 h in a water bath. The pH was then increased to 7–7.2 by the addition of 1 M NH_3, and incubated overnight at 28 °C to selectively precipitate the carrier ONC-DCless-H6, that is insoluble at neutral or alkaline pH values. The peptides were isolated from insoluble components by repeated cycles of centrifugation, and finally lyophilized. Their purity was checked by SDS/PAGE and mass spectrometry analyses. Lyophilized peptides were then dissolved in pure water, unless differently specified, and quantified by BCA assay (ThermoFisher Scientific, Waltham, MA).

2.5. Mass spectrometry analyses

Matrix-assisted laser desorption/ionisation mass spectrometry (MALDI-MS) was carried out on a 4800 Plus MALDI TOF/TOF mass spectrometer (Applied Biosystems, Framingham, MA) equipped with a nitrogen laser (337 nm). The peptide samples (1 mL) were mixed (1:1, v/v) with a 10 mg/mL solution of a-cyano-4-

hydroxycinnamic acid in acetonitrile/50 mM citrate buffer (70:30 v/v). Mass calibration was performed using external peptide standards purchased from Applied Biosystems, Framingham, MA. Spectra were acquired using 5,000 shots/spectrum in a mass (m/z) range of 1,000–5,000 amu and raw data were analysed using Data Explorer Software provided by the manufacturer.

2.6. Circular dichroism spectroscopy

CD experiments were performed on a Jasco J-815 circular dichroism spectropolarimeter, calibrated for intensity with ammonium [D10] camphorsulfonate ($[\theta_{290.5}] = 7{,}910$ deg cm^2 dmol^{-1}). The cell path length was 0.01 cm. CD spectra were collected at 25 °C in the 190–260 nm (far-UV) at 0.2 nm intervals, with a 20 nm/min scan rate, 2.5 nm bandwidth and a 16 s response. Spectra are reported in terms of mean residue ellipticity, calculated by dividing the total molar ellipticity by the number of amino acids in the molecule. Each spectrum was corrected by subtracting the background, and reported without further signal processing. Lyophilized peptides were dissolved in ultra-pure water (Romil, Waterbeach, Cambridge, GB) at a concentration of 100 μM, determined on the basis of peptide dry weight and BCA assay (ThermoFisher Scientific, Waltham, MA). CD spectra of the peptides were collected in the absence or in the presence of increasing concentrations of trifluoroethanol (TFE, Sigma Aldrich, Milan, Italy), SDS (Sigma Aldrich, Milan, Italy) or lipopolysaccharide (LPS) from *E.coli* 0111:B4 strain (Sigma Aldrich, Milan, Italy). CD spectra were corrected by subtracting every time the contribution of the compound under test at any given concentration. CD spectra deconvolution was performed by using the program PEPFIT, that is based on peptide-derived reference spectra [29], in order to estimate secondary structure contents. A Microsoft Excel-ported version of PEPFIT was used for convenience [30].

2.7. Measurement of IL-6 release

IL-6 levels were determined by ELISA assay (DuoSet ELISA kits, R&D Systems, Minneapolis, MN) following the manufacturer's instructions. Briefly, RAW 264.7 cells (5×10^4) were seeded into 96-well microtiter plates, and grown to semi-confluency. After 24 h, the culture medium was replaced with fresh medium containing the peptide under test (5 or 20 μM) in the presence or in the absence of LPS from *Salmonella Minnesota* (50 ng/mL, Sigma Aldrich, Milan, Italy) for 24 h at 37 °C. When the protective effect of peptides was evaluated, cells were pre-incubated with the peptide under test (5 or 20 μM) for 2 h at 37 °C. Following treatment, cells were washed three times with PBS prior to incubation with LPS (50 ng/mL) for further 24 h at 37 °C. In each case, at the end of incubation, the culture supernatants were collected, and centrifuged at 5,000 rpm for 3 min at room temperature, in order to remove cell debris. Samples were then analysed by reading absorbance values at 450 nm using 550 nm as a reference wavelength at an automatic plate reader (FLUOstar Omega, BMG LABTECH, Ortenberg, Germany).

2.8. Determination of NO production

To determine the levels of NO released by RAW 264.7 cells, a colorimetric assay based on the use of Griess reagent (Sigma Aldrich, Milan, Italy) was performed. The levels of nitrite (NO^{2-}) in cell supernatants were determined on the basis of a reference curve obtained by testing increasing concentrations (from 1 to 50 μM) of sodium nitrite dissolved in water. Briefly, cell culture supernatants were mixed with equal volumes of 1% sulphanilamide dissolved in 2.5% phosphoric acid, and incubated for 5 min at room temperature. Samples were then diluted 1:1 (v/v) with 0.1% N-(1-naphthyl) ethylenediamine dihydrochloride, and incubated for further 5 min at room temperature. Absorbance values were then determined at 520 nm using an automatic plate reader (FLUOstar Omega, BMG LABTECH, Ortenberg, Germany).

2.9. Antimicrobial activity assay

The antimicrobial activity of ApoB derived peptides was tested towards eight bacterial strains, *i.e. E. coli* ATCC 25922, methicillin-resistant *Staphylococcus aureus* (MRSA WKZ-2), *Salmonella enteriditis* 706 RIVM, *Bacillus globigii* TNO BM013, *Bacillus licheniformis* ATCC 21424, *Staphylococcus aureus* ATCC 29213, *Pseudomonas aeruginosa* ATCC 27853, and *Pseudomonas aeruginosa* PAO1. In each case, bacteria were grown to mid-logarithmic phase in MHB at 37 °C. Cells were then diluted to 2×10^6 CFU/mL in Nutrient Broth (Difco, Becton Dickinson, Franklin Lakes, NJ) containing increasing amounts of either r(P)ApoB$_L$ or r(P)ApoB$_S$ peptide (0,625–40 μM). In each case, starting from a peptide stock solution, twofold serial dilutions were sequentially carried out, accordingly to broth microdilution method [31]. Following overnight incubation, MIC_{100} values were determined as the lowest peptide concentration responsible for no visible bacterial growth.

2.10. Killing kinetics studies

To kinetically analyse bacterial killing by ApoB derived peptides, experiments were performed on *E. coli* ATTC 25922 and *Bacillus licheniformis* ATTC 21424 strains. To this purpose, bacteria were grown overnight in MHB medium, then diluted in fresh MHB, and incubated at 37 °C until logarithmic phase of growth was reached. Bacteria were then diluted to 4×10^6 CFU/mL in a final volume of 150 μL of Nutrient Broth 0.5X (Difco, Becton Dickinson, Franklin Lakes, NJ), and mixed with the peptide under test (1:1 v/v). For each strain, increasing concentrations of peptide were analysed (ranging from 0 to 20 μM or from 0 to 10 μM in the case of *E. coli* ATTC 25922 and *Bacillus licheniformis* ATTC 21424 strains, respectively). At defined time intervals, samples (20 μL) were serially diluted (from 10- to 10,000-fold), and 100 μL of each dilution was plated on TSA. Following an incubation of 16 h at 37 °C, bacterial colonies were counted.

2.11. Synergy evaluation

Synergism between ApoB derived peptides and antimicrobial agents was assessed by the so called "checkerboard" assay against *S. aureus* MRSA WKZ-2, *E. coli* ATCC 25922, *P. aeruginosa* ATCC 27853, *P. aeruginosa* PAO1, and *S. aureus* ATCC 29213 strains. To this purpose, ApoB derived peptides were tested in combination with EDTA or antibiotics, such as ciprofloxacin, colistin, erythromycin, kanamycin sulfate, and vancomycin. All these antimicrobial agents were from Sigma Aldrich, Milan, Italy. Twofold serial dilutions of each ApoB derived peptide and each antimicrobial agent were tested in combination on each strain tested. To do this, we tested peptide concentrations ranging from 0 to 20 μM. Compound concentrations tested on each strain are reported in Table 1. The fractional inhibitory concentration (FIC) index was calculated as follows: $FIC_A + FIC_B$, where FIC_A = MIC of drug A in combination/MIC of drug A alone, and FIC_B = MIC of drug B in combination/MIC of drug B alone. FIC indexes $\leqslant 0.5$ were classified as synergism, whereas FIC indexes between 0.5 and 4 were associated to additive or "no interaction" effects [32]. Antagonism is usually associated to a FIC index > 4.

Table 1
Range of antimicrobial agent concentrations tested on each strain for combination therapy analyses.

	S. aureus ATCC 29213	*S. aureus* MRSA WKZ-2	*P. aeruginosa* ATCC 27853	*P. aeruginosa* PAO1	*E. coli* ATCC 25922
Ciprofloxacin	0–0,5 μg/mL	0–1 μg/mL	0–2 μg/mL	0–1 μg/mL	0–0,03 μg/mL
Colistin	0–8 μg/mL	0–8 μg/mL	0–4 μg/mL	0–4 μg/mL	0–8 μg/mL
Erythromycin	0–4 μg/mL	0–4 μg/mL	0–16 μg/mL	0–128 μg/mL	0–128 μg/mL
Vancomycin	0–0,25 μg/mL	0–0,5 μg/mL	0–32 μg/mL	0–4 μg/mL	0–0,25 μg/mL
Kanamycin	0–0,5 μg/mL	0–0,125 μg/mL	0–64 μg/mL	0–8 μg/mL	0–0,125 μg/mL
EDTA	0–24,53 μg/mL	0–49,07 μg/mL	0–392,5 μg/mL	0–196,2 μg/mL	0–98,14 μg/mL

Each antimicrobial agent was tested for synergistic effects with ApoB derived peptides (0–20 μM) within the concentration range listed in the table, depending from the sensitivity of the specific bacterial strain.

2.12. Anti-biofilm activity

Anti-biofilm activity of ApoB derived peptides was tested on *S. aureus* MRSA WKZ-2, *E. coli* ATCC 25922, *P. aeruginosa* ATCC 27853, and *P. aeruginosa* PAO1 strains. Bacteria were grown overnight in MHB (Becton Dickinson Difco, Franklin Lakes, NJ), and then diluted to 1×10^8 CFU/mL in BM2 medium [33] containing increasing peptide concentrations (0–1 μM). Incubations with the peptides were carried out either for 4 h, in order to test peptide effects on biofilm attachment, or for 24 h, in order to test peptide effects on biofilm formation. When peptide effects on preformed biofilm were evaluated, bacterial biofilms were formed for 24 h at 37 °C, and then treated with increasing concentrations (0–1 μM) of the peptide under test. In all the cases, at the end of the incubation, the crystal violet assay was performed. To do this, the planktonic culture was removed from the wells, which were washed three times with sterile PBS prior to staining with 0.04% crystal violet (Sigma Aldrich, Milan, Italy) for 20 min. The colorant excess was eliminated by three successive washes with sterile PBS. Finally, the crystal violet was solubilised with 33% acetic acid and samples optical absorbance values were determined at 630 nm by using a microtiter plate reader (FLUOstar Omega, BMG LABTECH, Germany). To determine the percentage of viable bacterial cells inside the biofilm structure, upon biofilm disruption with 0,1% Triton X-100 (Sigma Aldrich, Milan, Italy), bacterial cells were ten-fold diluted on solid TSA and incubated for 16 h at 37 °C. Once evaluated the number of colony forming units, bacterial cell survival was calculated as follows: $(CFU_{\text{in treated sample}}/CFU_{\text{in untreated sample}}) \times 100$.

2.13. Cytotoxicity assays

Cytotoxic effects of ApoB derived peptides on RAW 264.7 cells were determined by using the cell proliferator reagent WST-1 (Roche Applied Science, Mannheim, Germany). To this purpose, RAW 264.7 cells were plated into 96-well plates at a density of 5×10^4 cells in 100 μL medium per well, and incubated overnight at 37 °C. Afterwards, cells were treated with increasing concentrations (0–20 μM) of the peptide under test for 24 h at 37 °C. Following incubation, peptide-containing medium was removed, and 100 μL of fresh medium containing 10% WST-1 reagent was added to each well. Following an incubation of 30 min at 37 °C in the dark, sample absorbance values were measured at 450 nm using 650 nm as a reference wavelength at a microtiter plate reader (FLUOstar Omega, BMG LABTECH, Germany).

Cytotoxic effects of peptides on the viability of malignant SVT2 murine fibroblasts, parental murine BALBc 3T3 fibroblasts, human HeLa cells, and human HaCaT keratinocytes were determined by using the 3-(4,5-dimethylthiazol-2-yl)-2,5-diphenyltetrazolium bromide (MTT) assay (Sigma Aldrich, Milan, Italy), as previously described [34]. Briefly, cells were seeded into 96-well plates at a density of 5×10^3/well in 100 μL medium per well, and incubated overnight at 37 °C. Afterwards, cells were treated with increasing concentrations (0–20 μM) of the peptide under test for 24 h at 37 °C. Following incubation, the peptide-containing medium was removed, and 100 μL of MTT reagent, dissolved in DMEM without phenol red (Sigma Aldrich, Milan, Italy), were added to the cells (100 μL/well) at a final concentration of 0.5 mg/mL. After 4 h at 37 °C, the culture medium was removed and the resulting formazan salts were dissolved by the addition of isopropanol containing 0.1 N HCl (100 μL/well). Absorbance values of blue formazan were determined at 570 nm using an automatic plate reader (Microbeta Wallac 1420, Perkin Elmer).

In all the cases, cell survival was expressed as the percentage of viable cells in the presence of the peptide under test, with respect to control cells grown in the absence of the peptide.

2.14. Haemolytic activity

The release of haemoglobin from mouse erythrocytes was used as a measure for the haemolytic activity of ApoB derived peptides. To do this, EDTA anti-coagulated mouse blood was centrifuged for 10 min at 800*g* at 20 °C, in order to obtain red blood cells (RBCs), which were washed three times, and 200-fold diluted in PBS. Subsequently, 75 μL aliquots of RBCs were added to 75 μL peptide solutions (final concentration ranging from 0 to 20 μM) in 96-well microtiter plates, and the mixture was incubated for 1 h at 37 °C. Following the incubation, the plate was centrifuged for 10 min at 1,300*g* at 20 °C, and 100 μL supernatant of each well were transferred to a new 96-well plate. Absorbance values were determined at 405 nm by using an automatic plate reader (FLUOstar Omega, BMG LABTECH, Germany), and the percentage of haemolysis was calculated by comparison with the control samples containing no peptide (negative control) or 0.2% (v/v) Triton X-100 (positive control, complete lysis). Haemolysis (%) = $[(Abs_{405\ nm}\ \text{peptide} - Abs_{405\ nm}\ \text{negative control})/(Abs_{405\ nm}\ 0.2\%\ \text{Triton} - Abs_{405\ nm}\ \text{negative control})] \times 100$.

2.15. Wound healing assay

Wound healing activity of r(P)ApoB$_L$ peptide was evaluated *in vitro* as previously described [35]. Human HaCaT keratinocytes were seeded into 12-well plates at a density of 6.3×10^5 cells/well in 1 mL medium per well. Following an incubation of 24 h at 37 °C, cells were pre-treated with 3 μM mitomycin C for 30 min, in order to inhibit cell proliferation [36]. Cell monolayers were then wounded with a pipette tip to remove cells from a specific region of the monolayer. The culture medium was then removed and the cells were washed twice with PBS. Cells were then incubated with fresh culture medium containing increasing concentrations of r(P)ApoB$_L$ peptide (0–0.5–10–20 μM). Wound closure was then followed by multiple field time-lapse microscopy (TLM) experiments, using an inverted microscope (Zeiss Axiovert 200, Carl Zeiss, Germany) equipped with an incubator to control temperature, humidity and CO_2 percentage [37,38]. Images were iteratively acquired in phase contrast with a CCD video camera (Hamamatsu

Orca AG, Japan) by using a 5× objective. The microscope was also equipped with a motorized stage and focus control (Marzhauser, Germany) enabling automated positioning of the acquired samples. The workstation was controlled through a homemade software in Labview. Each cell sample was analysed in duplicate, and in any case at least two fields of view were selected. Since three independents experiments were carried out, from 8 to 12 independent fields of view were analysed for each sample. The delay between consecutive imaging of the same field of view was set to 15 min. The wound closure dynamics were quantified by using a homemade automated image analysis software, that allowed to measure the size of the wound area for each time point (A). For each field of view, determined values were normalized with respect to the value of the wound area at time 0 (A_0), and plotted as function of time. After an initial lag phase, the wound area was found to decrease with a constant velocity [39,40]. By reporting A/A_0 values as a function of time, a linear decrease was observed for A/A_0 values lower than 0.8 (Fig. 9b). For each sample, the lag time t_L was calculated as the time required to obtain an initial wound closure corresponding to $A/A_0 = 0.8$. Being R^2 typically higher than 0.98, the linear range of the curve was fitted, and the slope ($-\alpha$) was considered a measure of the wound closure velocity. The values of wound closure velocity obtained for each field of view from three independent experiments were averaged (α), and normalized with respect to the value of the corresponding control sample (α_{contr}). For each peptide concentration tested, α/α_{contr} values obtained from three independent experiments were averaged and the standard error of the mean was calculated to account for reproducibility [41].

2.16. Statistical analysis

Statistical analysis was performed using a Student's *t*-Test. Significant differences wereindicated as $^{*}(P < 0.05)$, $^{**}(P < 0.01)$ or $^{***}(P < 0.001)$.

3. Results

3.1. Recombinant production of ApoB derived peptides

Expression of HDPs in bacterial cells can be deleterious to the host due to their toxicity. For this reason, we used a procedure to produce HDPs as fusion proteins with onconase (ONC), a frog ribonuclease that mediates the delivery to inclusion bodies very efficiently, as previously described [24,27], thus avoiding toxicity problems. DNA sequences encoding peptide ApoB887-923 or

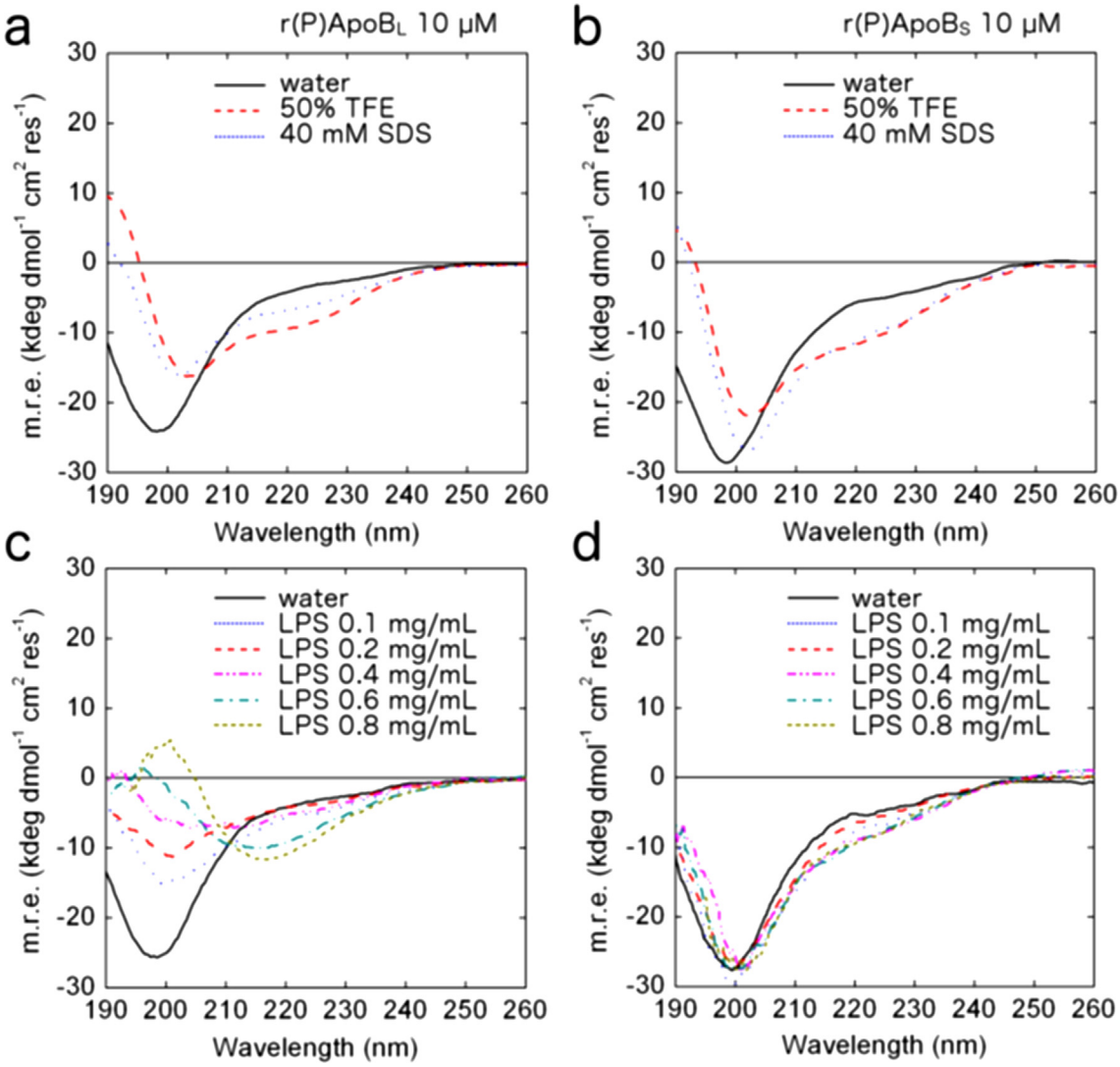

Fig. 2. Far-UV CD spectra of recombinant peptides r(P)ApoB$_L$ (a, c) and r(P)ApoB$_S$ (b, d) at a concentration of 10 μM in the presence of increasing concentrations of membrane-mimicking agents TFE or SDS at micellar concentrations (a, b) or of LPS (c, d).

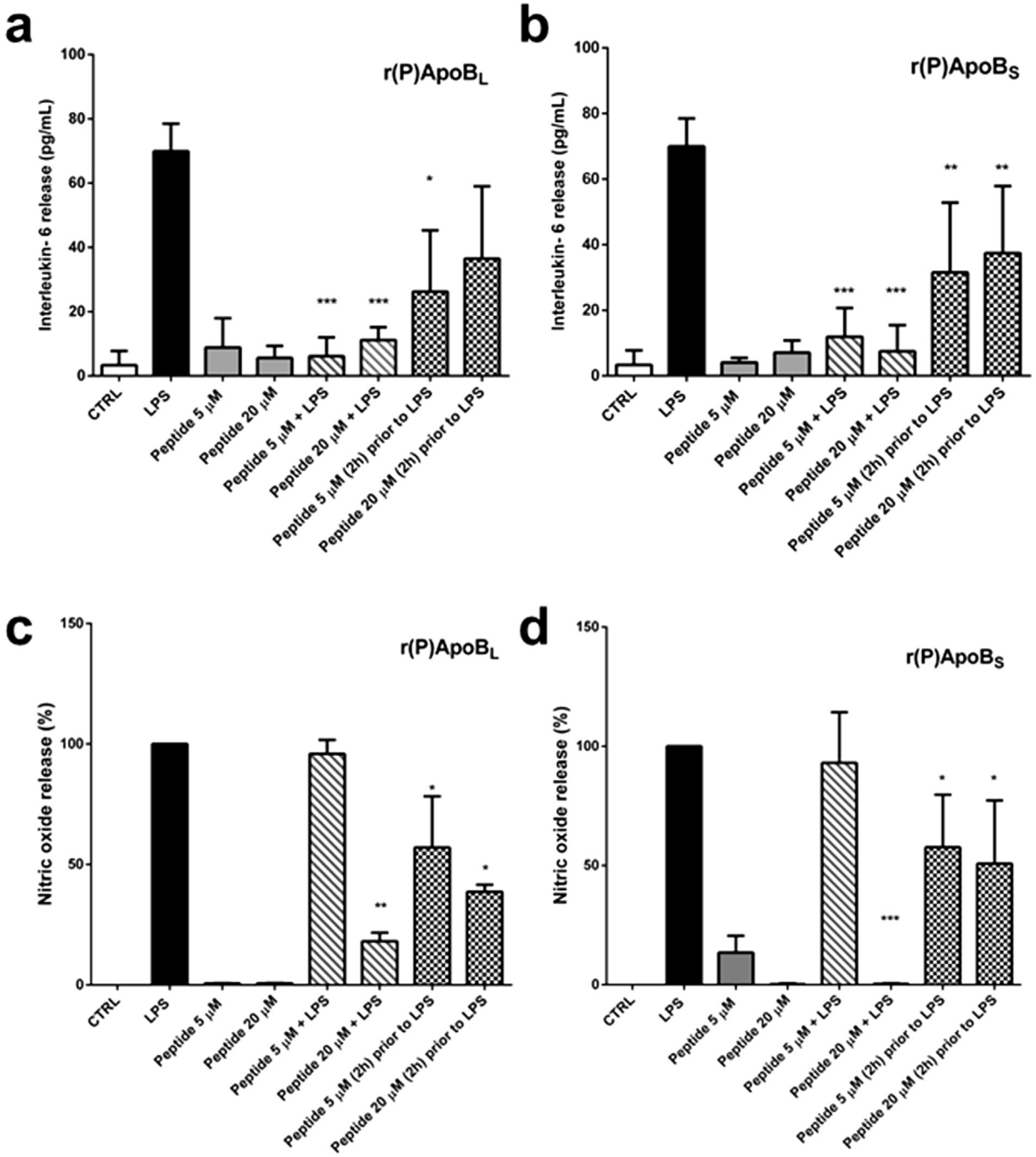

Fig. 3. Effects of ApoB derived peptides on the release of IL-6 (a, b) and NO (c, d) in mouse macrophages RAW 264.7 stimulated with LPS (50 ng/mL) from *Salmonella Minnesota*. The effects of r(P)ApoB$_L$ (a, c) and r(P)ApoB$_S$ (b, d) peptides were evaluated either co-incubating cells with the peptide under test (5 or 20 μM) and LPS (oblique grey lanes) or by treating cells with the peptide under test (5 or 20 μM) for 2 h at 37 °C prior to incubation with LPS (chessboard bars). Results were compared to those obtained in the case of control untreated cells (white bars), cells stimulated with the LPS alone (black bars), or cells incubated with two different concentrations (5 or 20 μM) of peptide (grey bars). Data represent the mean (±standard deviation, SD) of at least three independent experiments, each one carried out with triplicate determinations. $^{*}P < 0.05$, $^{**}P < 0.01$, or $^{***}P < 0.001$ were obtained for control *versus* treated samples.

peptide ApoB887-911, synthesized by MWG Biotech in conformity with the *E. coli* codon usage, were cloned into the expression vector pET22b(+), downstream to a sequence encoding a mutated form of ONC. The resulting fusion proteins contain a His tag sequence, positioned between the ONC and the peptide moieties, suitable for an easy purification of the fusion protein, a flexible linker (Gly-Thr-Gly), and a dipeptide (Asp-Pro), which is cleaved in mild acidic conditions thus allowing the release of the peptide from the carrier. Since the carrier is insoluble at neutral or alkaline pH, ApoB derived peptides were isolated from insoluble components by repeated cycles of centrifugation, and finally lyophilized. Peptides' purity was checked by SDS/PAGE and matrix assisted laser desorption ionisation (MALDI) mass spectrometry analyses. Recombinant peptides were found to be 99% pure. Molecular mass values of ApoB887-923 and ApoB887-911 were found to be 4,072.3 Da (Theoretical MH^+ 4072.7) and 2,820.9 Da (Theoretical MH^+ 2820.2), respectively, values which are in agreement with the expected molecular weights of the peptides with the addition of a Pro

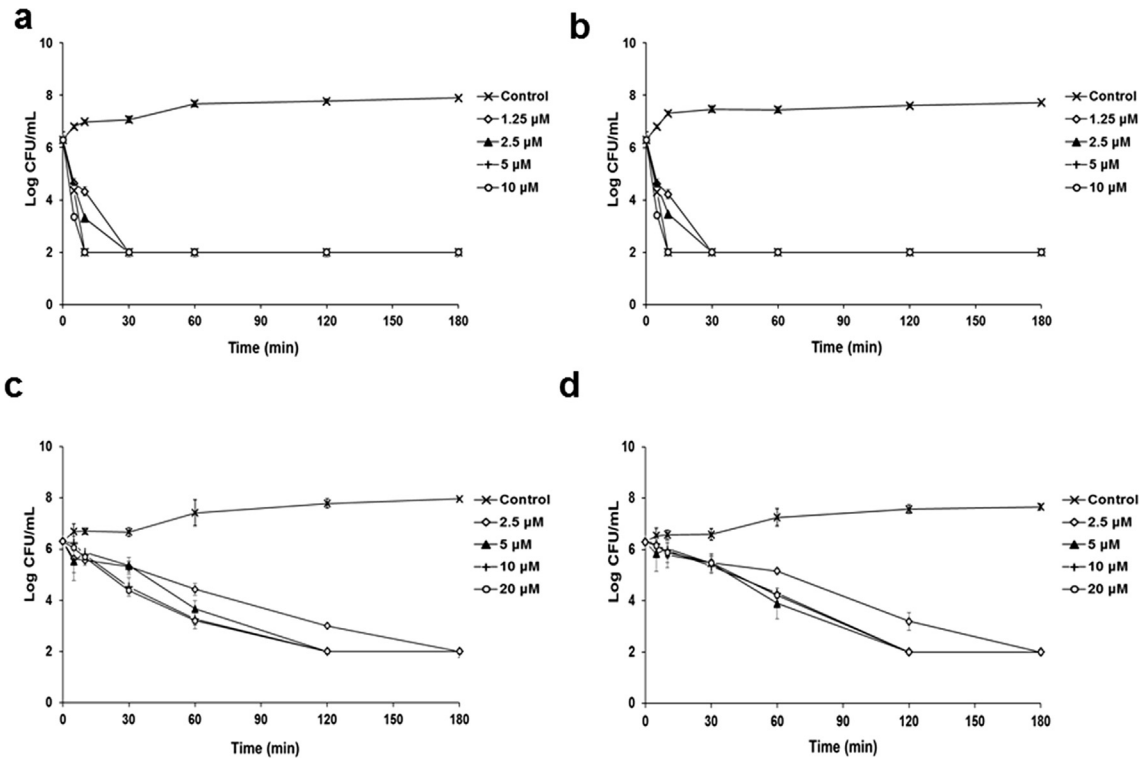

Fig. 4. Time killing curves obtained by incubating *Bacillus licheniformis* ATTC 21424 (a, b) and *E. coli* ATTC 25922 (c, d) strains with increasing concentrations of r(P)ApoB$_L$ (a, c) or r(P)ApoB$_S$ (b, d) peptides for different lengths of time. Data represent the mean (±standard deviation, SD) of at least three independent experiments, each one carried out with triplicate determinations.

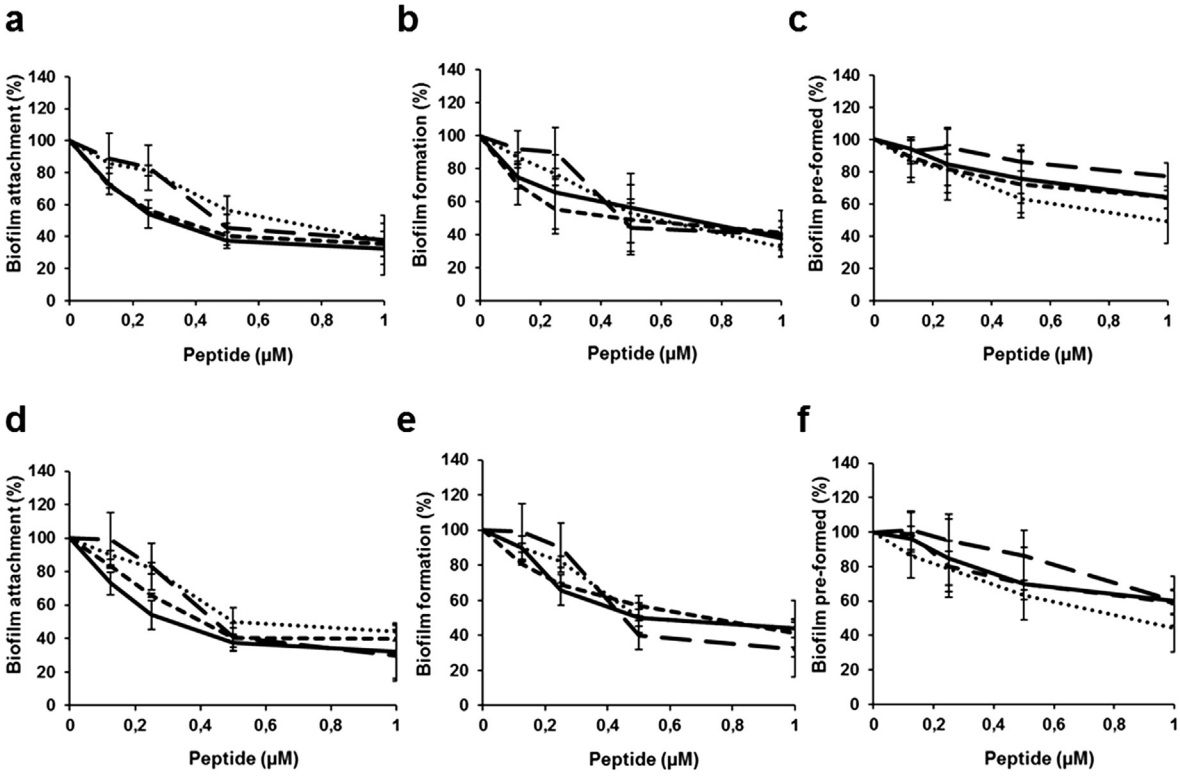

Fig. 5. Anti-biofilm activity of r(P)ApoB$_L$ (–), r(P)ApoB$_S$ (---), CATH-2 (– – –), and LL-37 (●●●) peptides on *E. coli* ATCC 25922 (a, b, c) and *S. aureus* MRSA WKZ-2 (d, e, f) strains in BM2 medium. The effects of increasing concentrations of peptides were evaluated either on biofilm attachment (a, d), biofilm formation (b, e), or on pre-formed (c, f) biofilm. Biofilm was stained with crystal violet and measured at 630 nm. Data represent the mean (±standard deviation, SD) of at least three independent experiments, each one carried out with triplicate determinations. For all the experimental points, $^{*}P < 0.05$, $^{**}P < 0.01$, or $^{***}P < 0.001$ were obtained for control *versus* treated samples.

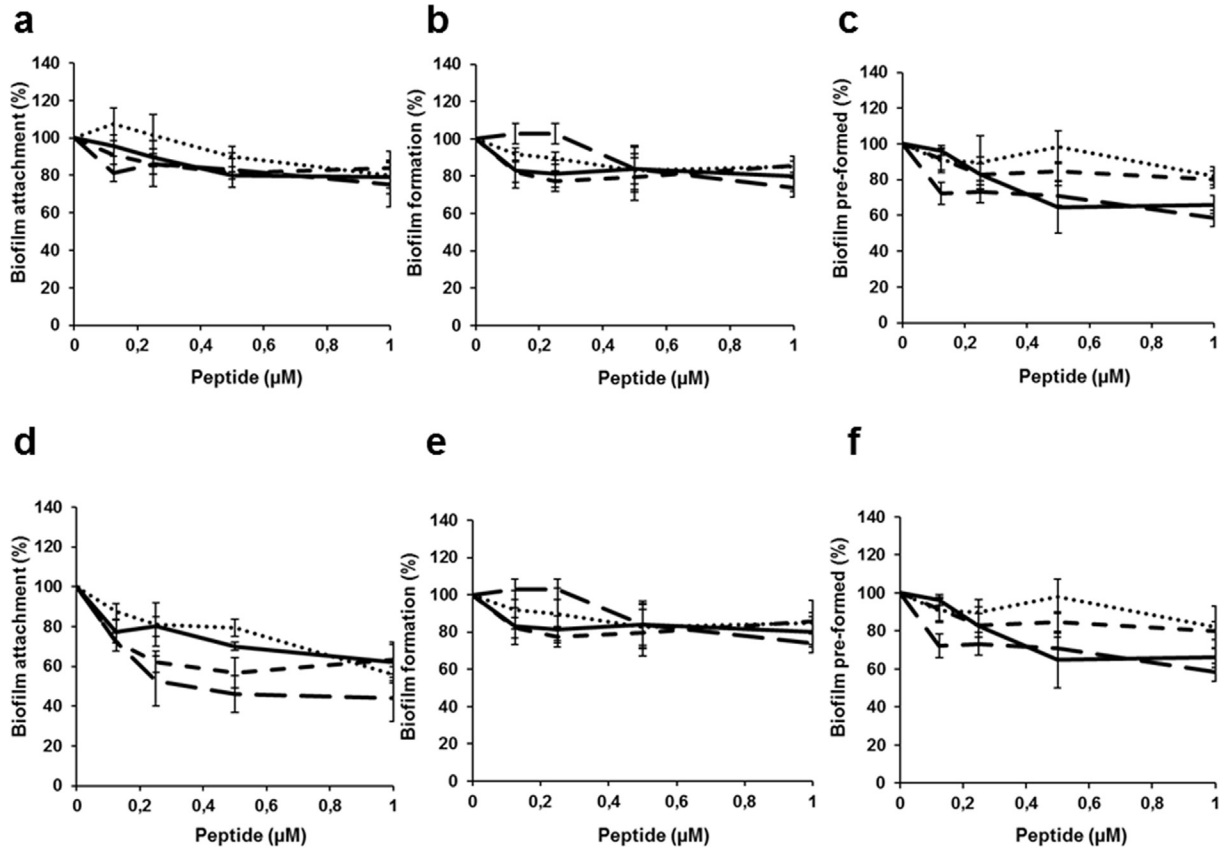

Fig. 6. Anti-biofilm activity of r(P)ApoB$_L$ (–), r(P)ApoB$_S$ (---), CATH-2 (– – –), and LL-37 (•••) peptides on *P. aeruginosa* ATCC 27853 (a, b, c) and *P. aeruginosa* PAO1 (d, e, f) strains in BM2 medium. The effects of increasing concentrations of peptides were evaluated either on biofilm attachment (a, d), biofilm formation (b, e), or on pre-formed (c, f) biofilm. Biofilm was stained with crystal violet and measured at 630 nm. Data represent the mean (±standard deviation, SD) of at least three independent experiments, each one carried out with triplicate determinations. For all the experimental points, $^{*}P < 0.05$, or $^{**}P < 0.01$ were obtained for control *versus* treated samples.

residue deriving from the cleavage of the Asp-Pro bond. The final yield of peptides ApoB887-923 and ApoB887-911, here named r(P)ApoB$_L$ and r(P)ApoB$_S$, was about 7 and 4 mg/L of bacterial culture, respectively.

3.2. Conformational analyses of r(P)ApoB$_L$ and r(P)ApoB$_S$ peptides by Far-UV circular dichroism

To analyse the secondary structure of recombinant ApoB derived peptides, we performed Far-UV CD spectra, and found that both peptides are largely unstructured in pure water (Fig. 2a and b). We also evaluated the effects of membrane-mimicking agents, such as TFE and SDS at micellar concentrations, on peptide conformation. We found that r(P)ApoB$_L$ secondary structure shifts mainly towards an α-helical conformation in presence of both membrane-mimicking agents, and only a partial (<10%) increase in β-strand content is observed (Table 2). This is clearly evidenced by the presence of two broad minima at around 208 and 222 nm, and a maximum at <200 nm (Fig. 2a). A similar behavior has been described for different HDPs [24,42,43], and suggests that r(P)ApoB$_L$ peptide is prone to assume a specific ordered conformation when interacting with membrane-mimicking agents. Similar effects, even if significantly less pronounced, were observed in the case of r(P)ApoB$_S$ peptide (Fig. 2b and Table 2). No appreciable β-strand formation was observed for this peptide, probably indicating that, in the r(P)ApoB$_L$ peptide, β-strand propensity is mainly localized in the C-terminus region.

We also analysed by CD spectroscopy the effects of the endotoxin LPS (lipopolysaccharide), the predominant glycolipid in the outer membrane of Gram-negative bacteria [44], on the peptide conformations (Fig. 2c and d and Table 2). When r(P)ApoB$_L$ secondary structure was analysed in the presence of increasing concentrations (from 0.1 to 0.8 mg/mL) of *E. coli* LPS, the progressive appearance of a maximum at approximately 200 nm and of a minimum at approximately 218 nm suggested that the peptide tends to assume a prevalently β-strand conformation, probably induced by its interaction with LPS (Fig. 2c and Table 2). As expected on the basis of previous analyses, in which r(P)ApoB$_S$ does not show any β-strand content, no significant effects were observed in the case of r(P)ApoB$_S$ (Fig. 2d and Table 2) under the experimental conditions tested.

3.3. Analysis of the immunomodulatory activity of r(P)ApoB$_L$ and r(P)ApoB$_S$ peptides

Based on CD analyses, we hypothesized that an interaction between r(P)ApoB$_L$ peptide and LPS occurs. Since it is widely reported that HDPs are able to mitigate the pro-inflammatory effects induced by endotoxins [45], we tested the anti-inflammatory properties of ApoB derived peptides by monitoring their effects on LPS induced interleukin-6 (IL-6) release, as well as on nitric oxide (NO) release in murine macrophages (RAW 264.7 cell line). In fact, it is known that, upon activation by internal and external stimuli, macrophages produce and secrete various endogenous inflammatory mediators, such as nitric oxide (NO) and pro-inflammatory cytokines, including interleukin-6 [46,47].

To test the effects of ApoB derived peptides on the release of IL-6, ELISA assays were performed on LPS stimulated RAW 264.7 cells. As shown in Fig. 3a and b, a significant release of IL-6 was observed in control cells incubated with LPS from *Salmonella*

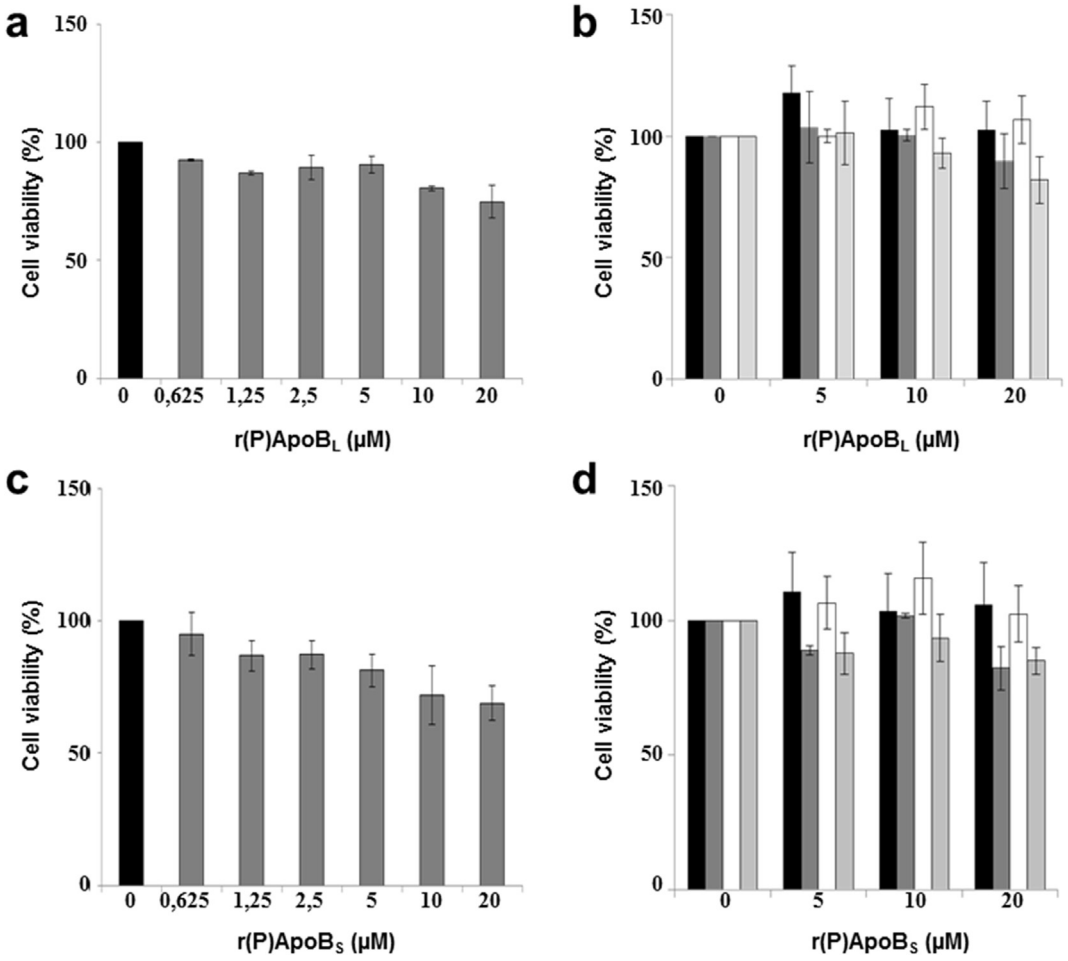

Fig. 7. Effects of r(P)ApoB$_L$ (a, b) and r(P)ApoB$_S$ (c, d) peptides on the viability of RAW 264.7 (a, c), BALBc3T3 (black bars in b, d), SVT2 (dark grey bars in b, d), Hela (white bars in b, d), and HaCaT (light grey bars in b, d) cells. Cell viability was assessed by WST-1 (a, c) or MTT (b, d) assay, and expressed as the percentage of viable cells with respect to controls (untreated cells). Error bars indicate standard deviations obtained from at least three independent experiments, each one carried out with triplicate determinations.

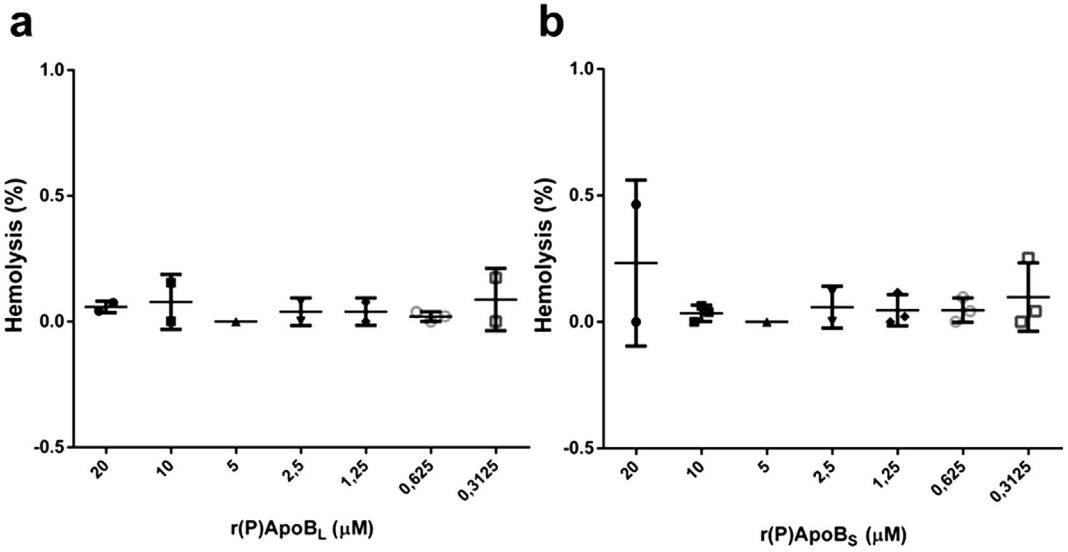

Fig. 8. Haemolytic activity of r(P)ApoB$_L$ (a) and r(P)ApoB$_S$ (b) peptides towards murine red blood cells (RBCs) after 1 h of incubation at 37 °C. Data represent the mean (±standard deviation, SD) of at least three independent experiments, each one carried out with triplicate determinations.

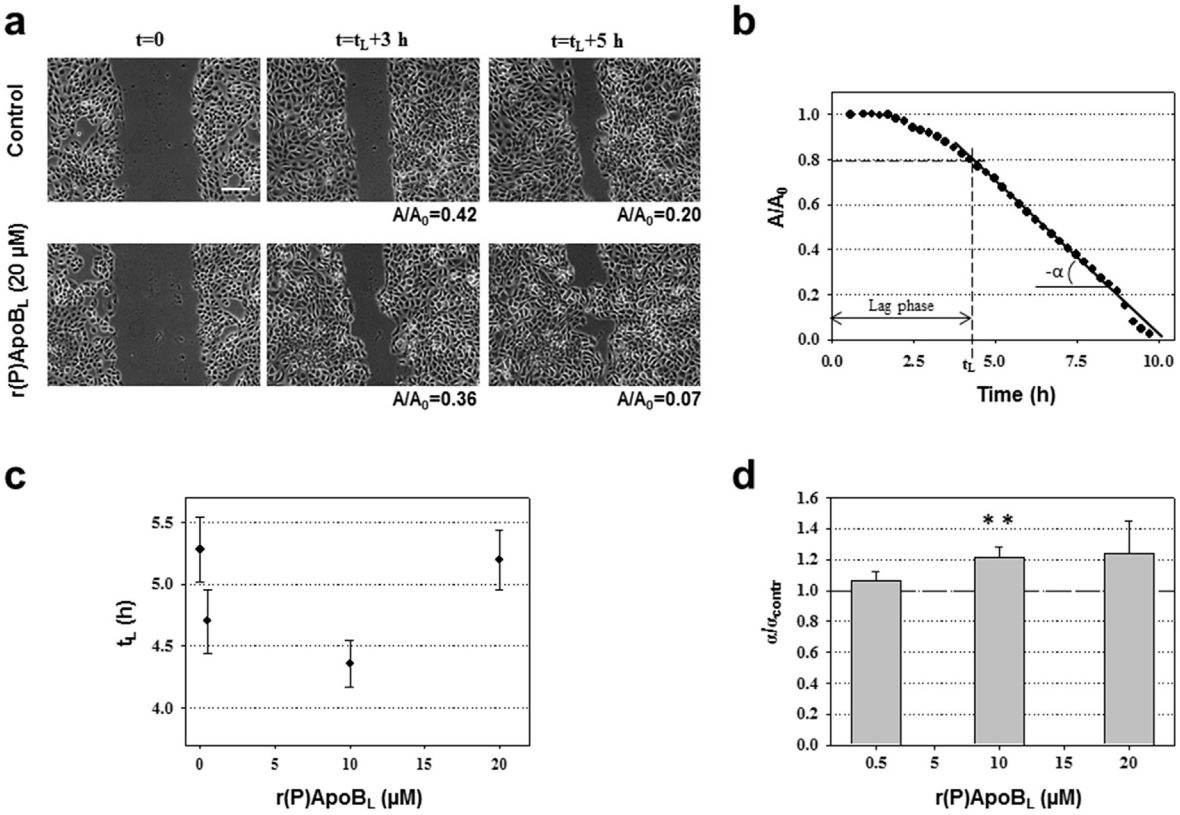

Fig. 9. Wound healing activity of r(P)ApoB$_L$ peptide on HaCaT cells monolayer. Cells were pre-treated for 30 min with 3 μM mitomycin C, and then wounded prior to incubation with r(P)ApoB$_L$ peptide (0.5–10–20 μM) for 12 h at 37 °C. Images were acquired for untreated HaCaT cells and for cells treated with 20 μM peptide (a). The lag phase time (t_L) corresponds to the time interval before the linear decrease of the wound area. Images were acquired at time t = 0 (a, on the left), 3 h after t_L (a, in the middle) and 5 h after t_L (a, on the right). For each sample, A/A_0 values are reported, where A is the wound area after a specific incubation time and A_0 is the wound area at time 0. Scale bar = 150 μm. In (b), evolution in time of the wound area (A), normalized with respect to A_0, is reported for a control sample. A homemade automated image analysis software was used to measure the size of the cell-free area (A) for each time point. For A/A_0 values < 0.8, a linear correlation with the incubation time was found. The slope $-\alpha$ of the linear fit, reported as a continuous line, represents a measure of the wound closure velocity. In (c), determined t_L values are reported as a function of peptide concentration (0–0.5–10–20 μM). In (d), wound closure velocity (α), normalized with respect to control sample (α_{contr}), is reported as a function of peptide concentration (0.5–10–20 μM). The dashed line corresponds to $\alpha/\alpha_{contr} = 1$. In (c) and (d), each data point represents the mean (±standard error) of three independent experiments. $^{**}P < 0.01$ was obtained for control *versus* treated samples.

Table 2
Analysis of r(P)ApoB$_L$ and r(P)ApoB$_S$ peptides secondary structure.

	H_2O			TFE		
	α-Helix (%)	β-Strand (%)	Random coil (%)	α-Helix (%)	β-Strand (%)	Random coil (%)
r(P)ApoB$_L$	5	12	83	26	18	56
r(P)ApoB$_S$	7	3	90	26	0	74
	SDS			LPS		
	α-Helix (%)	β-Strand (%)	Random coil (%)	α-Helix (%)	β-Strand (%)	Random coil (%)
r(P)ApoB$_L$	17	21	62	11	64	25
r(P)ApoB$_S$	29	3	68	18	2	80

Secondary structure content of ApoB derived peptides in water and in the presence of trifluoroethanol (TFE), sodium dodecyl sulfate (SDS), and lipopolysaccharide (LPS), calculated by means of PEPFIT program.

Minnesota (50 ng/mL). When murine macrophages were incubated with LPS (50 ng/mL) in the presence of either r(P)ApoB$_L$ (Fig. 3a) or r(P)ApoB$_S$ (Fig. 3b) peptide (two different peptide concentrations), a strong decrease of IL-6 release was observed with respect to LPS induced control cells. Moreover, we found that both peptides have a significant protective effect on LPS stimulated RAW 264.7 cells. In fact, when macrophages were pre-treated for 2 h with either r(P)ApoB$_L$ or r(P)ApoB$_S$ peptide and then incubated for further 24 h with LPS, a significant decrease of IL-6 release was observed (Fig. 3a and b).

Similar results were observed when the effects of ApoB derived peptides were tested on NO release (Fig. 3c and d). Also in this case, following co-incubation of cells with LPS from *Salmonella Minnesota* and either r(P)ApoB$_L$ or r(P)ApoB$_S$ peptide, a significant attenuation of NO release with respect to control cells was detected (Fig. 3c and d). However, in this case, it has to be noticed that a significant effect of peptides on NO release was observed only at the highest peptide concentration tested (20 μM), while at 5 μM concentration both peptides were found to be almost ineffective (Fig. 3c and d). However, when RAW 264.7 cells were

pre-treated for 2 h with 5 or 20 μM of either r(P)ApoB$_L$ or r(P)ApoB$_S$ peptide and subsequently stimulated for 24 h with LPS (50 ng/mL), a significant reduction of NO release was observed even at 5 μM peptide concentration (Fig. 3c and d), thus confirming the protective effect of both peptides on LPS stimulated RAW 264.7 cells.

3.4. Antimicrobial activity of r(P)ApoB$_L$ and r(P)ApoB$_S$ peptides

The antibacterial activity of recombinant ApoB derived peptides was determined by measuring their MIC$_{100}$ values on a panel of Gram-negative and Gram-positive bacterial strains (Table 3). A significant antimicrobial activity of r(P)ApoB$_L$ and r(P)ApoB$_S$ peptides was detected towards four out of eight strains tested, *i.e. E. coli* ATCC 25922, *P. aeruginosa* PAO1, *B. globigii* TNO BM013, and *B. licheniformis* 21424, for which almost identical MIC$_{100}$ values were calculated for both ApoB derived peptides. Notably, MIC$_{100}$ values were found to be comparable or even significantly lower than those determined when control cathelicidin-2 (CATH-2), a known HDP from chicken [48], was tested (Table 3). These data indicate that r(P)ApoB$_L$ and r(P)ApoB$_S$ peptides are endowed with a broad-range antimicrobial activity, being effective on both Gram-negative and Gram-positive bacterial strains. On the other hand, ApoB derived peptides were found to be ineffective towards *P. aeruginosa* ATCC 27853, methicillin-resistant *S. aureus* (MRSA WKZ-2), and *S. aureus* 29213 (Table 3), while, in the case of *S. enteriditis* 706 RIVM, a significant antibacterial effect was elicited only by r(P)ApoB$_L$ peptide.

To analyse the kinetic of peptides bactericidal activity, kinetic killing curves were obtained by treating *E. coli* ATTC 25922 and *B. licheniformis* ATTC 21424 strains, highly susceptible to both peptides (Table 3), with increasing concentrations of either r(P)ApoB$_L$ or r(P)ApoB$_S$ for different times (0–180 min). We found that, at the highest peptide concentrations tested (5–10 μM), *B. licheniformis* cells were killed within 10 min, while at the lowest peptide concentrations (1.25–2.5 μM) the same effect was obtained within 30 min (Fig. 4a and b). When peptides were tested on *E. coli* ATTC 25922 at high concentrations (5–10-20 μM), bacterial cells were killed within 120 min, while at the lowest peptide concentration (2.5 μM) the same effect was obtained within 180 min (Fig. 4c and d).

3.5. Combination therapy analyses

To potentiate the antimicrobial efficacy of recombinant ApoB derived peptides for therapeutic purposes, especially against *P. aeruginosa* and *S. aureus* strains, we carried out combination therapy analyses by concomitantly administrating peptides and antibiotics in various combinations to bacteria. One of the best known tests to evaluate synergism between two compounds is the so called "chequerboard" experiment, in which a two-dimensional array of serial concentrations of test compounds is used as the basis for calculation of a fractional inhibitory concentration (FIC) index to demonstrate that paired combinations of agents can exert inhibitory effects that are more than the sum of their effects alone [32]. It is generally accepted that FIC indexes $\leqslant$0.5 are indicative of "synergy"; FIC indexes comprised between >0.5 and 4.0 are, instead, associated to "additive" or "no interaction" effects, whereas FIC indexes >4.0 are indicative of "antagonism" [32].

As reported in Table 4, all the combinations tested were found to be effective, either with additive or synergistic effects between peptides and antibiotics. Notably, no FIC indexes higher than 2 were measured.

The most potent combinations were obtained in the presence of EDTA, which was selected for its ability to affect bacterial outer membrane permeability, thus sensitizing bacteria to a number of antibiotics [49–51]. Very pronounced synergistic effects were observed for both ApoB derived peptides in combination with EDTA on *S. aureus* MRSA WKZ-2 and both *P. aeuroginosa* strains.

Both peptides were found to act synergistically with (i) ciprofloxacin on all the strains tested (Table 4); (ii) colistin on all the strains tested, except for *S. aureus* ATTC 29213 (Table 4); (iii) vancomycin on *S. aureus* MRSA WKZ-2, *P. aeruginosa* strains and *E. coli* ATTC 25922 (Table 4); (iv) erythromycin on *P. aeruginosa* ATCC

Table 3
Antibacterial activity of ApoB derived peptides.

	MIC$_{100}$ (μM) r(P)ApoB$_L$	r(P)ApoB$_S$	CATH-2
Gram-negative strains			
Escherichia coli ATCC 25922	10	10	10
Pseudomonas aeruginosa ATCC 27853	>40	>40	10
Pseudomonas aeruginosa PAO1	20	20	20
Salmonella enteriditis 706 RIVM	10	>40	10
Gram-positive strains			
Staphilococcus aureus MRSA WKZ-2	>40	>40	10
Bacillus globigii TNO BMO13	5	2.5	5
Bacillus licheniformis ATCC 21424	1.25	1.25	20
Staphylococcus aureus ATCC 29213	>40	>40	10

Minimum Inhibitory Concentration (MIC, μM) values determined for r(P)ApoB$_L$ and r(P)ApoB$_S$ peptides tested on a panel of Gram-positive and Gram-negative bacterial strains. Chicken CATH-2 peptide was used as a positive control. Values were obtained from a minimum of three independent experiments.

Table 4
Combination therapy analyses.

Bacterial strains	Antibiotic	ΣFICI[a] r(P) ApoB$_L$	r(P) ApoB$_S$
Methicillin resistant *S. aureus MRSA WKZ-2*	Ciprofloxacin	0,328	0,365
	Colistin	0,340	0,350
	Erythromycin	1,094	1,375
	Vancomycin	0,425	0,316
	Kanamycin	2,000	0,387
	EDTA	0,278	0,360
S. aureus ATTC 29213	Ciprofloxacin	0,340	0,413
	Colistin	1,049	1,024
	Erythromycin	1,049	1,146
	Vancomycin	1,049	1,097
	Kanamycin	1,049	0,352
	EDTA	1,049	0,351
P. aeruginosa ATCC 27853	Ciprofloxacin	0,347	0,328
	Colistin	0,267	0,255
	Erythromycin	0,389	0,170
	Vancomycin	0,379	0,306
	Kanamycin	0,479	1,030
	EDTA	0,333	0,089
P. aeruginosa PAO1	Ciprofloxacin	0,396	0,444
	Colistin	0,144	0,266
	Erythromycin	0,569	0,556
	Vancomycin	0,500	0,486
	Kanamycin	0,507	0,389
	EDTA	0,396	0,438
E. coli ATCC 25922	Ciprofloxacin	0,363	0,442
	Colistin	0,438	0,292
	Erythromycin	1,243	1,292
	Vancomycin	0,428	0,426
	Kanamycin	0,603	0,572
	EDTA	0,729	0,750

Fractional inhibitory concentration (FIC) indexes determined for r(P)ApoB$_L$ and r(P)ApoB$_S$ peptides tested in combination with antibiotics or EDTA on Gram-positive and Gram-negative bacterial strains. Indexes were obtained from a minimum of three independent experiments, each one carried out with triplicate determinations.

27853 (Table 4). In the latter case, a FIC index of 0.38 and 0.17 for r(P)ApoB$_L$ and r(P)ApoB$_S$ peptides, respectively, was obtained. In the case of kanamycin, the response varied depending on the peptide and the specific bacterial strain. In fact, r(P)ApoB$_L$ was found to act synergistically with this antibiotic prevalently on Gram-negative bacteria, particularly on the *P. aeruginosa* strains, whereas r(P)ApoB$_S$ peptide was found to be very active in the presence of kanamycin against both *S. aureus* strains as well as against *P. aeruginosa* PAO1 strain (FIC indexes < 0.4).

It should be emphasized that combinations of ApoB derived peptides with antibiotics or EDTA were found to have a strong antimicrobial activity also towards strains on which the peptides alone were found to be ineffective, such as both *S. aureus* strains and *P. aeruginosa* ATCC 27853 (Table 3). Notably, we did not observe any antagonistic interactions between the peptides and the antimicrobials under test.

3.6. Anti-biofilm activity of r(P)ApoB$_L$ and r(P)ApoB$_S$ peptides

Anti-biofilm peptides represent a very promising approach to treat biofilm-related infections and have an extraordinary ability to interfere with various stages of the biofilm growth mode [52]. To test whether recombinant ApoB derived peptides are endowed with anti-biofilm activity, we performed experiments on different bacterial strains, such as *E. coli* ATCC 25922, *Pseudomonas aeruginosa* PAO1, *Pseudomonas aeruginosa* ATCC 27853, and methicillin-resistant *Staphylococcus aureus* MRSA WKZ-2 in BM2 medium. The same experiments were also performed using LL-37 control peptide, that is a human antimicrobial peptide known to have a significant anti-biofilm activity against multidrug-resistant bacterial strains [53]. We also tested for the first time CATH-2 anti-biofilm activity. Three different approaches were followed. At first, we tested the peptide effects on biofilm attachment. To do this, the bacterial culture, following overnight growth, was diluted in BM2 medium containing increasing concentrations of the peptide under test (0–1 μM), and incubated for 4 h at 37 °C. Following incubation, biofilm analysis by crystal violet staining revealed a significant dose-dependent inhibition of biofilm attachment in the case of *E. coli* ATCC 25922 (Fig. 5a) and *S. aureus* MRSA WKZ-2 (Fig. 5d) strains treated with r(P)ApoB$_L$ (continuous line in Fig. 5a, d) or r(P)ApoB$_S$ (smaller dashed line in Fig. 5a, d) peptides. Similar results were obtained on these two strains in the case of peptides CATH-2 (larger dashed line in Fig. 5a, d) and LL-37 (dotted line in Fig. 5a, d). Strong effects were also displayed by ApoB derived peptides on biofilm attachment in the case of *P. aeruginosa* PAO1 strain (Fig. 6d). A less pronounced effect of ApoB derived peptides (about 20% inhibition of biofilm formation) was observed, instead, on *P. aeruginosa* ATCC 27853 biofilm attachment (Fig. 6a).

Second, we tested the effect of ApoB derived peptides on biofilm formation. To investigate this phenomenon, we followed the experimental procedure described above with the only exception that bacterial cells were incubated with increasing concentrations of peptides for 24 h at 37 °C. Also in this case, we observed a significant dose-dependent inhibition of biofilm formation in the case of *E. coli* ATCC 25922 (Fig. 5b) and *S. aureus* MRSA WKZ-2 (Fig. 5e) strains treated with r(P)ApoB$_L$ (Fig. 5b, e) or r(P)ApoB$_S$ (Fig. 5b, e) peptides. Similar effects were elicited by peptides CATH-2 (Fig. 5b, e) and LL-37 (Fig. 5b, e). ApoB derived peptides strongly affected also *P. aeruginosa* PAO1biofilm formation (Fig. 6e). In the case of *P. aeruginosa* ATCC 27853, instead, a less pronounced effect (about 20% biofilm formation inhibition) was observed for all the peptides under test (Fig. 6b).

Third, we tested the effect of ApoB derived peptides on preformed biofilms. By incubating preformed biofilms of *E. coli* ATCC 25922 (Fig. 5c) and *S. aureus* MRSA WKZ-2 (Fig. 5f) strains with increasing concentrations of r(P)ApoB$_L$ (Fig. 5c, f) or r(P)ApoB$_S$ (Fig. 5c, f), we found a significant reduction (about 50%), an effect even stronger than that observed in the case of CATH-2 peptide (Fig. 5c, f). Similar results were observed in the case of *P. aeruginosa* PAO1 strain (Fig. 6f). On the other hand, when the peptides were tested on *P. aeruginosa* ATCC 27853 preformed biofilm, a slight effect (about 20% reduction) was observed for all the peptides except for CATH-2, which was found to have a strong effect (about 50% reduction, Fig. 6c).

We also evaluated the percentage of viable bacterial cells inside the biofilm structure by colony counting assay. We found that, even at the highest ApoB derived peptides concentrations tested, a significant percentage of bacterial cells appeared to be still alive (Table 5). Similar results were also obtained in the case of LL-37 and CATH-2 control peptides on both *P. aeruginosa* strains (Table 5), even if it has to be noticed that, in the case of biofilm formation, both control peptides affected the viability of *P. aeruginosa* PAO1 cells more than ApoB derived peptides (Table 5). CATH-2 and LL-37 control peptides were also found to strongly impair the viability of *E. coli* ATCC 25922 and *S. aureus* MRSA WKZ-2 cells in the case of biofilm eradication (Table 5).

3.7. Biocompatibility of r(P)ApoB$_L$ and r(P)ApoB$_S$ peptides

The development of HDPs as therapeutic agents is strictly related to their selective toxicity towards bacterial cells [54]. The presence of zwitterionic phospholipids and cholesterol on the

Table 5
Effects of peptides on the viability of bacterial cells inside the biofilm structure.

	In biofilm attachment (%)				In biofilm formation (%)				In biofilm eradication (%)			
	r(P)ApoB$_L$	r(P)ApoB$_S$	CATH-2	LL-37	r(P)ApoB$_L$	r(P)ApoB$_S$	CATH-2	LL-37	r(P)ApoB$_L$	r(P)ApoB$_S$	CATH-2	LL-37
***E. coli* ATCC 25922**	105±7	101±9	15±5	97±8	79±7	79±9	40±3	73±12	83±14	80±5	15±2	37±6
MRSA WKZ-2	90±7	102±9	35±5	70±4	66±7	60±8	23±3	69±12	66±11	70±3	10±2	17±6
***P. aeruginosa* ATCC 27853**	76±11	68±10	91±5	60±13	66±13	64±14	96±16	77±15	70±15	59±9	59±12	69±5
***P. aeruginosa* PAO1**	52±12	77±15	45±7	47±7	55±14	57±14	35±16	25±14	44±15	86±6	50±10	58±9

Effects of r(P)ApoB$_L$, r(P)ApoB$_S$, CATH-2, and LL-37 peptides (1 μM) on the viability of bacterial cells inside the biofilm structure. To determine the percentage of viable bacterial cells, biofilm was lysed with Triton X-100 (0,1%), bacterial cells were ten-fold diluted, and colonies were counted after an incubation of 16 h at 37 °C. Data are expressed as percentage with respect to control untreated samples, and represent the mean (±standard deviation, SD) of at least three independent experiments, each one carried out with triplicate determinations. For all the experimental points, $^{*}P < 0.05$, or $^{**}P < 0.01$ were obtained for control *versus* treated samples.

outer leaflet of eukaryotic cell membranes largely accounts for the preference of HDPs for bacterial membranes over eukaryotic membranes [55,56]. To deepen on the therapeutic potential of ApoB derived peptides, we analysed their cytotoxic effects towards a panel of mouse and human eukaryotic cells. The addition of increasing concentrations (from 0.625 to 20 μM) of ApoB derived peptides to mouse macrophages Raw 264.7 cells for 24 h did not result in any significant reduction in cell viability (Fig. 7a and c). A slight toxicity was detected only at the highest peptide concentrations tested (10 and 20 μM in Fig. 7a and c). We also tested ApoB derived peptides on murine embryo fibroblasts BALBc 3T3 and their tumor counterpart, *i.e.* SVT2 simian virus 40-transformed cell line (Fig. 7b and d). A slight toxicity (10–20%) was detected only in the case of SVT2 cells at the highest concentration tested (20 μM in Fig. 7b and d). Moreover, no significant toxic effects were detected when ApoB derived peptides were assayed on human cervical cancer HeLa cells (Fig. 7b and d), while a slight toxicity (~20%) was observed in the case of human keratinocytes (HaCaT cells) at the highest concentration (20 μM in Fig. 7b and d). ApoB derived peptides were also tested on murine red blood cells (RBCs) to exclude haemolytic effects. As shown in Fig. 8, both peptides did not exert any lytic effect on mouse RBCs, even at the highest concentration tested (20 μM).

3.8. Wound healing activity of r(P)ApoB$_L$ peptide

Numerous studies support the hypothesis that human HDPs promote wound healing in skin, by modulating cytokine production, cell migration, proliferation and, in some cases, angiogenesis [57]. Based on this, we performed experiments to test whether r(P)ApoB$_L$ peptide is able to stimulate wound re-epithelialization by human keratinocytes (HaCaT cell line). To this purpose, we performed a classical *in vitro* wound healing assay to evaluate peptide effects on cell migration. HaCaT cell monolayers were pre-treated with 3 μM mitomycin C for 30 min, and then wounded with a pipette tip to remove cells from a specific region of the monolayers. Cells were then washed with PBS and incubated with r(P)ApoB$_L$ (0, 0.5, 10, and 20 μM). As it is well known that the spreading of cells in the wound area is due to two mechanisms, *i.e.* cell motility and cell proliferation [37,40,58], a pre-treatment with mitomycin C allowed us to exclude any influence of cell proliferation on the wound healing process.

In Fig. 9a, we reported the images acquired during a time-lapse wound healing experiment on control cells, and on cells treated with 20 μM r(P)ApoB$_L$ peptide at three time points, *i.e.* at time 0 and at 3 and 5 h after the lag time (t_L), defined as a transient time period (t_L) before the linear decrease of the wound area (see below). By the comparison of the images of treated and untreated cells at each time point, it emerged that the cells treated with 20 μM peptide were able to close the wound faster than the control cells. In order to quantify the wound closure, we used an automated image analysis software, that allowed us to measure the size of the cell-free area (A) for each time point. The obtained values were normalized with respect to the value measured at time 0 (A_0) for each field of view, and plotted as a function of time (Fig. 9b). In Fig. 9a, at t = 5 h after t_L, A/A_0 values were found to be 0.20, and 0.07 for the control sample, and for the cells treated with 20 μM peptide, respectively. This evidence suggests that r(P)ApoB$_L$ peptide might be able to stimulate wound re-epithelialization by human keratinocytes. As shown in Fig. 9b, where A/A_0 values of control cells are reported as a function of time, after an initial lag phase (t_L), the wound area decreases with a constant velocity. The initial lag phase, corresponding to a transient time period (t_L) before the linear decrease of the wound area, has been observed for all the analysed samples, and has been found to range between 3 and 5 h independently from peptide concentrations under test (Fig. 9c).

As the slope (α) of the line represents the measure of the wound closure velocity, each α value calculated in the presence of the peptide was normalized with respect to the value calculated for untreated cells (α_{contr}), and plotted as a function of peptide concentration (Fig. 9d). It appeared that the cells treated with the peptide show an increased wound closure velocity with respect to the control cells ($\alpha/\alpha_{contr} > 1$). In particular, in the case of the cells treated with 10 μM peptide, an increment of about 20% in the normalized wound closure velocity ($\alpha/\alpha_{contr} = 1.21$, data statistically significant) was observed. When cells were treated with 20 μM peptide, a slightly higher value of the normalized wound closure velocity was measured ($\alpha/\alpha_{contr} = 1.23$). However, in the latter case, a higher data variability was observed (larger error bar), leading to a limited statistical significance of the result.

Overall, our results indicate that r(P)ApoB$_L$ peptide is able to promote the migration and the consequent wound healing in HaCaT keratinocyte monolayers when tested at concentration values ranging between 0.5 and 20 μM.

4. Discussion

Recently, an abundance of multidrug-resistant bacteria has emerged, whereas very few classes of new antibiotics have been discovered. The knowledge that HDPs may prevent infections in many organisms opened interesting perspectives to the applications of these peptides as a new class of antimicrobials. In fact, they initially attracted attention solely for their direct antimicrobial activity, and were studied as promising alternative antibiotic candidates due to their prospective potency, rapid action, and broad spectrum of activity against Gram-negative and Gram-positive bacteria, viruses, fungi and parasites [59,60]. To date, more than 1,000 natural cationic HDPs with antimicrobial properties have been identified [61]. These peptides constitute a major component of the ancient, nonspecific innate defence system in most multicellular organisms [3,19,59,60]. However, it has to be emphasized that most natural HDPs have, indeed, modest direct antimicrobial activities, and exhibit multiple mechanisms of action, with a consequent low potential to induce *de novo* resistance [59]. This class of peptides includes both the bioactive peptides displaying direct antimicrobial activity and those that stimulate the immune system to clear or prevent an infection [59,61]. In mammals, the expression of mature and biologically active HDPs requires a proteolytic cleavage event determining the release of the "cryptic" bioactive peptide from its precursor protein [62]. In fact, it should be emphasized that a wide variety of human proteins, whose primary functions are not necessarily related to host defence, contain HDPs hidden inside their sequences [63,64]. Fascinatingly, human proteome could be seen as a yet unexplored source of bioactive peptides with potential pharmacological applications. In this context, apolipoproteins have been identified as a source of bioactive peptides displaying broad anti-infective and antiviral activities [22]. Indeed, the presence of antiviral peptides hidden within apolipoprotein sequences may be related to the fact that lipoproteins and viruses share a similar cell biological niche, having a comparable size and displaying similar interactions with mammalian cells and receptors [22]. ApoB is one of the several apolipoproteins that play key roles in lipoprotein metabolism [65], and represents the ligand for receptor-mediated removal of low density lipoprotein particles from circulation [65]. ApoB contains two LDL (low-density lipoprotein) receptor binding domains, namely region A (ApoB3147-3157) and region B (ApoB3359-3367), which is more uniformly conserved across species and that has been found to be endowed with a significant antiviral activity

[22]. Moreover, ApoB derived peptides have been already used in vaccine preparations to treat atherosclerosis [23]. Here, we applied our *in silico* analysis method to a human ApoB isoform [26,27] and identified a novel "cryptic" HDP (region 887–922). To the best of our knowledge, this ApoB region has never been analysed before, since all the previously identified biologically active ApoB peptides are far from the high scoring region identified in the present work [22,23]. By applying our *in silico* analysis, we identified an absolute maximum score, corresponding to region 887–922 (Fig. 1), and a relative maximum score, corresponding to residues 887–909 (Fig. 1). Here, we focused our attention on these two ApoB sequences by producing in bacterial cells two recombinant HDPs, here named r(P)ApoB$_L$ and (P)ApoB$_S$, 38- and 26-residue long, respectively. Both recombinant peptides were found to exhibit antibacterial activities against both Gram-positive and Gram-negative strains, including the pathogenic strains *P. aeruginosa* PAO1 and *B. globigii* TNO BM013, while having negligible cytotoxic effects on a panel of human and murine cell lines. Time killing curves also indicated that peptides exert a strong bactericidal activity against susceptible strains. However, it has to be underlined that ApoB derived peptides were found to be ineffective towards *P. aeruginosa* ATCC 27853, methicillin-resistant *S. aureus* (MRSA WKZ-2), and *S. aureus* ATTC 29213 strains, while, in the case of *S. enteriditis* 706 RIVM strain, a significant antibacterial effect was displayed only by r(P)ApoB$_L$ peptide. This observation is in agreement with previous findings indicating that most natural cationic antimicrobial peptides do not appear to be highly optimized for direct antimicrobial activity, since it is likely that multiple modestly active peptides with concomitant immunomodulatory activities work effectively in combination and/or when induced or delivered to sites of infection [66]. Indeed, considering this, we performed combination therapy analyses and found that both ApoB derived peptides are able to synergistically act with either commonly used antibiotics or EDTA, the latter selected for its ability to affect bacterial outer membrane permeability, thus sensitizing bacteria to a number of antibiotics [49–51]. Interestingly, synergistic effects were observed towards most of the strains under test, including methicillin-resistant *S. aureus* MRSA WKZ-2, on which peptides alone were found to be ineffective even at high concentrations (40 μM). Although the use of a single agent to treat pathogens is the most common practice in clinics, combination therapy approaches have several advantages, such as low potential to induce resistant phenotype, efficacy at lower drug doses, with a consequent mitigation of toxic effects, and possibility to target a broad spectrum of pathogens [67]. Interestingly, both r(P)ApoB$_L$ and r(P)ApoB$_S$ peptides showed synergism with systemic antibiotic ciprofloxacin against all the strains under test (FIC indexes ranging from 0.3 to 0.44). This would allow to significantly lower the doses of the antibiotic in the combination therapy approaches, with a consequent decrease of the appearance of resistant clinical isolates, an undesired phenomenon strongly affecting ciprofloxacin efficacy [68]. ApoB derived peptides also showed synergistic effects with colistin and vancomycin against most of the strains under test (FIC indexes ranging from 0.14 to 0.5). Since both colistin and vancomycin are responsible for toxic effects at high concentrations [67,69], a combination therapeutic approach based on a reduced frequency of antibiotic administration and/or exposure to antibiotic may offer several advantages over conventional dosing schemes. However, the most potent synergism was observed for both ApoB derived peptides in combination with EDTA, with FIC indexes ranging from 0.089 to 0.4. In the case of *P. aeruginosa* strains, synergism might be associated to EDTA ability to combine with magnesium ions playing a key role in the self-interaction of LPS molecules, with a consequent LPS release determining an increased permeability of bacterial membrane [50]. This might ultimately facilitate peptide internalization into bacterial cells, thus potentiating the peptide antimicrobial activity. EDTA is also known to determine the release of endogenous phospholipases, with a consequent alteration of Gram-negative bacteria outer membrane [70]. In the case of *S. aureus* strains, the increase of bacterial membrane permeability might be due to the ability of EDTA to solubilize extracellular polymeric substances [71], mainly composed by exopolysaccharides and playing a key role in biofilm establishment.

It should be highlighted that, although in some cases FIC indexes very close to 0.5 make it difficult to discriminate between synergistic and additive effects, no antagonistic interactions were observed between peptides and antimicrobials. Furthermore, combinations of ApoB derived peptides with antibiotics and EDTA were found to have a strong antimicrobial activity also towards strains on which the peptides alone were found to be ineffective, such as both *S. aureus* strains and *P. aeruginosa* ATCC 27853, indicating that in drug combinations a reciprocal facilitation and potentiation of different mechanisms of action is realized.

Interestingly, ApoB derived peptides are also endowed with anti-biofilm activity. Microorganisms growing in a biofilm state are very resilient to the treatment by many antimicrobial agents. Indeed, biofilm infections are a significant problem in chronic and long-term infections, including those colonizing medical devices and implants [52]. Specific cationic HDPs have recently been described to have multispecies anti-biofilm activity, which is independent of their activity against planktonic bacteria [9]. We found that ApoB derived peptides are effective on biofilm formation and biofilm attachment, and, even more interestingly, they strongly affect pre-formed biofilms. Furthermore, ApoB derived peptides display anti-biofilm activity even on bacterial strains not sensitive to the peptide antimicrobial activity, such as *S. aureus* MRSA WKZ-2, and, in the case of sensitive strains, even at peptide concentrations (0.625–1 μM) significantly lower than those required to directly kill planktonic cells. This is in agreement with previous reports indicating that LL-37 peptide potently inhibits the formation of bacterial biofilms *in vitro* at the very low and physiologically meaningful concentration of 0.5 μg/mL, significantly lower than that required to kill or inhibit bacterial growth (64 μg/mL) [72]. As a consequence of this, it should be emphasized that even at the highest ApoB derived peptides concentrations tested, a significant percentage of bacterial cells inside the biofilm structure appeared to be still alive. This was observed for both ApoB derived peptides and LL-37 control peptide, while it was less pronounced in the case of CATH-2 peptide. Based on this, it is tempting to speculate that successful therapeutic approaches could be designed by combining anti-biofilm peptides and conventional antibiotics ineffective on biofilm, but effective on bacterial cells entrapped into the biofilm structure.

From a structural point of view, by Far UV-CD analyses, we found that ApoB derived peptides are unstructured in aqueous buffer, and tend to assume a conformation in the presence of membrane mimicking agents. In the presence of increasing concentrations of LPS, r(P)ApoB$_L$ peptide was found to gradually assume a defined structure, what suggests a direct binding of this peptide to LPS. This was not observed, instead, in the case of r(P)ApoB$_S$ peptide. It has also to be highlighted that both r(P)ApoB$_L$ and r(P)ApoB$_S$ peptides are endowed with immunomodulatory activities by significantly decreasing the release of pro-inflammatory IL-6 and NO in LPS induced murine RAW 264.7 macrophages. Both ApoB derived peptides were found to efficiently act either when the cells were co-incubated with the peptide under test in the presence of LPS or when the cells were pre-treated with the peptide for 2 h and then incubated with LPS for further 24 h, thus indicating that both peptides are able to display a significant protective action. However, it has to be noticed that, differently from r(P)ApoB$_L$ peptide, r(P)ApoB$_S$ was found to play anti-

inflammatory activities, when co-incubated with LPS, only at the highest peptide concentration tested (20 μM), whereas both r(P)$ApoB_S$ concentrations (5 and 20 μM) were found to efficiently exert a protective effect. This might be due to the fact that ApoB derived peptides probably act through different mechanisms, with r(P)$ApoB_L$ peptide mainly acting by binding to LPS and consequently interfering with its activity on target cells, and r(P)$ApoB_S$ peptide mainly acting on cell membrane and competing with LPS for the binding to specific cell sites. Therefore, a complex picture emerges, in agreement with the observation that HDPs immunomodulatory activities are extremely diverse [14]. Further experiments will allow us to elucidate the molecular mechanisms at the basis of ApoB derived peptides anti-inflammatory effects, which might include multiple aspects, such as stimulation of chemotaxis, suppression of bacterial induced pro-inflammatory cytokine production, regulation of neutrophil and epithelial cell apoptosis, modulation of cellular differentiation pathways, and promotion of angiogenesis and wound healing. As for the last aspect, in agreement with previous findings on LL-37 human peptide [73,74], we found that r(P)$ApoB_L$ peptide is able to stimulate human keratinocytes wound re-epithelialization *in vitro*, an evidence that opens new and interesting perspectives on future topical applications of this human HDP.

It has to be underlined that, although there are very few HDPs currently in use in the market, many are progressing through clinical trials that have focused on topic rather than systemic treatment because of peptides potential toxicity. However, it is conceivable that judicious formulations of HDPs for a clinical use, *e.g.* peptide inclusion in liposomal nanoparticles, will avoid undesired toxicity and degradation, thus allowing a sustainable HDPs delivery [18]. Here, we show that both ApoB derived peptides are not toxic for eukaryotic cells and do not determine any haemolytic effect when tested on murine red blood cells. These observations associated to their multifunctional properties and to their ability to synergistically act in combination with conventional antibiotic drugs open interesting perspectives to their therapeutic applications.

Conflict of interest statement

None declared.

Acknowledgements

We acknowledge “Programma di scambi internazionali con Università ed Istituti di ricerca stranieri per la mobilità di breve durata di docenti, ricercatori e studiosi” of the University of Naples Federico II, that financially supported scientific exchanges between Universities of Naples and Utrecht. The technical expert assistance by Dr. Johanna L. M. Tjeerdsma-van Bokhoven is acknowledged.

References

[1] M.T. Parker, J.H. Hewitt, Methicillin resistance in Staphylococcus aureus, Lancet 1 (1970) 800–804.
[2] J.N. Pendleton, S.P. Gorman, B.F. Gilmore, Clinical relevance of the ESKAPE pathogens, Exp. Rev. Anti Infect. Ther. 11 (2013) 297–308.
[3] M. Zasloff, Antimicrobial peptides of multicellular organisms, Nature 415 (2002) 389–395.
[4] D.A. Phoenix, S.R. Dennison, F. Harris, Antimicrobial Peptides: Their History, Evolution, and Functional Promiscuity, Wiley, 2013.
[5] R.E. Hancock, R. Lehrer, Cationic peptides: a new source of antibiotics, Trends Biotechnol. 16 (1998) 82–88.
[6] J.D. Hale, R.E. Hancock, Alternative mechanisms of action of cationic antimicrobial peptides on bacteria, Exp. Rev. Anti Infect. Ther. 5 (2007) 951–959.
[7] E.C. Spindler, J.D. Hale, T.H. Jr Giddings, R.E. Hancock, R.T. Gill. Deciphering the mode of action of the synthetic antimicrobial peptide Bac8c, Antimicrob. Agents Chemother. 55 (2012) 1706–1716.
[8] C.D. Fjell, J.A. Hiss, R.E. Hancock, G. Schneider, Designing antimicrobial peptides: form follows function, Nat. Rev. Drug Discov. 11 (2012) 37–51.
[9] C. de la Fuente-Nunez, F. Reffuveille, E.F. Haney, S.K. Straus, R.E. Hancock, Broad-spectrum anti-biofilm peptide that targets a cellular stress response, PLoS Pathog. 10 (2014) e1004152.
[10] A.F.G. Cicero, F. Fogacci, A. Colletti, Potential role of bioactive peptides in prevention and treatment of chronic diseases: a narrative review, Br. J. Pharmacol. (2016), http://dx.doi.org/10.1111/bph.13608.
[11] R.E.W. Hancock, M.G. Scott, The role of antimicrobial peptides in animal defences, Proc. Natl. Acad. Sci. U.S.A. 97 (2000) 8856–8861.
[12] D. Yang, A. Biragyn, D.M. Hoover, J. Lubkowski, J.J. Oppenheim, Multiple roles of antimicrobial defensins, cathelicidins, and eosinophil-derived neurotoxin in host defense, Annu. Rev. Immunol. 22 (2004) 181–215.
[13] D. Yang, A. Biragyn, L.W. Kwak, J.J. Oppenheim, Mammalian defensins in immunity: more than just microbicidal, Trends Immunol. 23 (2002) 291–296.
[14] A.T.Y. Yeung, S.L. Gellatly, R.E.W. Hancock, Multifunctional cationic host defence peptides and their clinical applications, Cell. Mol. Life Sci. 68 (2011) 2161–2176.
[15] D.M. Easton, A. Nijnik, M.L. Mayer, R.E.W. Hancock, Potential of immunomodulatory host defense peptides as novel anti-infectives, Trends Biotechnol. 27 (2009) 582–590.
[16] T.A. Waldmann, Immunotherapy: past, present and future, Nat. Med. 9 (2003) 269–277.
[17] J. Kindrachuk, E. Scruten, S. Attah-Poku, K. Bell, A. Potter, L.A. Babiuk, P.J. Griebel, S. Napper, Stability, toxicity, and biological activity of host defense peptide BMAP28 and its inversed and retro-inversed isomers, Biopolymers 96 (2011) 14–24.
[18] M. Sobczak, C. Dębek, E. Olędzka, R. Kozłowski, Polymeric systems of antimicrobial peptides – strategies and potential applications, Molecules 18 (2013) 14122–14137.
[19] K.L. Brown, R.E.W. Hancock, Cationic host defense (anti-microbial) peptides, Curr. Opin. Immunol. 18 (2006) 24–30.
[20] E. Guaní-Guerra, T. Santos-Mendoza, S.O. Lugo-Reyes, L.M. Terán, Antimicrobial peptides: general overview and clinical implications in human health and disease, Clin. Immunol. 135 (2010) 1–11.
[21] N. Mookherjee, R.E.W. Hancock, Cationic host defence peptides: innate immune regulatory peptides as a novel approach for treating infections, Cell. Mol. Life Sci. 64 (2007) 922–933.
[22] B.A. Kelly, I. Harrison, Á. McKnight, C.B.B. Dobson, Anti-infective activity of apolipoprotein domain derived peptides in vitro: identification of novel antimicrobial peptides related to apolipoprotein B with anti-HIV activity, BMC Immunol. 11 (2010) 13.
[23] C. Pierides, A. Bermudez-Fajardo, G.N. Fredrikson, J. Nilsson, E. Oviedo-Orta, Immune responses elicited by apoB-100-derived peptides in mice, Immunol. Res. 56 (2013) 96–108.
[24] K. Pane, V. Sgambati, A. Zanfardino, G. Smaldone, V. Cafaro, T. Angrisano, E. Pedone, S. Di Gaetano, D. Capasso, E.F. Haney, V. Izzo, M. Varcamonti, E. Notomista, R.E. Hancock, A. Di Donato, E. Pizzo, A new cryptic cationic antimicrobial peptide from human apolipoprotein E with antibacterial activity and immunomodulatory effects on human cells, FEBS J. 283 (2016) 2115–2131.
[25] E. Notomista, A. Falanga, S. Fusco, L. Pirone, A. Zanfardino, S. Galdiero, M. Varcamonti, E. Pedone, P. Contursi, The identification of a novel Sulfolobus islandicus CAMP-like peptide points to archaeal microorganisms as cell factories for the production of antimicrobial molecules, Microb. Cell Fact. 14 (2015) 126.
[26] S.H. Chen, C.Y. Yang, P.F. Chen, D. Setzer, M. Tanimura, W.H. Li, A.M. Gotto, L. Chan, The complete cDNA and amino acid sequence of human apolipoprotein B-100, J. Biol. Chem. 261 (1986) 12918–12921.
[27] C.Y. Yang, Z.W. Gu, S.A. Weng, T.W. Kim, S.H. Chen, H.J. Pownall, P.M. Sharp, S. W. Liu, W.H. Li, A.M. Jr, Gotto. Structure of apolipoprotein B-100 of human low density lipoproteins, Arteriosclerosis 9 (1989) 96–108.
[28] K. Pane, L. Durante, E. Pizzo, M. Varcamonti, A. Zanfardino, V. Sgambati, A. Di Maro, A. Carpentieri, V. Izzo, A. Di Donato, V. Cafaro, E. Notomista, Rational design of a carrier protein for the production of recombinant toxic peptides in Escherichia coli, PLoS ONE 11 (2016) e0146552.
[29] J. Reed, T.A. Reed, A set of constructed type spectra for the practical estimation of peptide secondary structure from circular dichroism, Anal. Biochem. 254 (1997) 36–40.
[30] M.A. Amon, M. Ali, V. Bender, K. Hall, M.-I. Aguilar, J. Aldrich-Wright, N. Manolios, Kinetic and conformational properties of a novel T-cell antigen receptor transmembrane peptide in model membranes, Peptide Sci. 14 (2008) 714–724.
[31] I. Wiegand, K. Hilpert, R.E. Hancock, Agar and broth dilution methods to determine the minimal inhibitory concentration (MIC) of antimicrobial substances, Nat. Protoc. 3 (2008) 163–175.
[32] F.C. Odds, Synergy, antagonism, and what the chequerboard puts between them, J. Antimicrob. Chemother. 52 (2003) 1.
[33] J. Li, T. Kleintschek, A. Rieder, Y. Cheng, T. Baumbach, U. Obst, T. Schwartz, P.A. Levkin, Hydrophobic liquid-infused porous polymer surfaces for antibacterial applications, ACS Appl. Mater Interfaces 5 (2013) 6704–6711.
[34] A. Arciello, N. De Marco, R. Del Giudice, F. Guglielmi, P. Pucci, A. Relini, D.M. Monti, R. Piccoli, Insights into the fate of the N-terminal amyloidogenic polypeptide of ApoA-I in cultured target cells, J. Cell Mol. Med. 15 (2011) 2652–2663.

[35] C.C. Liang, A.Y. Park, J.L. Guan, In vitro scratch assay: a convenient and inexpensive method for analysis of cell migration in vitro, Nat. Protoc. 2 (2007) 329–333.
[36] A. Di Grazia, F. Cappiello, A. Imanishi, A. Mastrofrancesco, M. Picardo, R. Paus, M.L. Mangoni, The frog skin-derived antimicrobial peptide esculentin-1a(1–21)NH2 promotes the migration of human HaCaT keratinocytes in an EGF receptor-dependent manner: a novel promoter of human skin wound healing? PLoS ONE 10 (2015) e0128663.
[37] F. Ascione, S. Caserta, S. Guido, Wound healing revisited: a transport phenomena approach, Chem. Eng. Sci. 160 (2017) 200–209.
[38] F. Ascione, A. Vasaturo, S. Caserta, V. D'Esposito, P. Formisano, S. Guido, Comparison between fibroblast wound healing and cell random migration assays in vitro, Exp. Cell Res. 347 (2016) 123–132.
[39] A.Q. Cai, K.A. Landman, B.D. Hughes, Multi-scale modeling of a wound-healing cell migration assay, J. Theor. Biol. 245 (2007) 576–594.
[40] P.K. Maini, D.L.S. McElwain, D.I. Leavesley, Traveling wave model to interpret a wound-healing cell migration assay for human peritoneal mesothelial cells, Tissue Eng. 10 (2004) 475–482.
[41] G. Cumming, F. Fidler, D.L. Vaux, Error bars in experimental biology, J. Cell Biol. 177 (2007) 7–11.
[42] A.P. Subasinghage, D. O'Flynn, J.M. Conlon, C.M. Hewage, Conformational and membrane interaction studies of the antimicrobial peptide alyteserin-1c and its analogue [E4K]alyteserin-1c, Biochim. Biophys. Acta 2011 (1808) 1975–1984.
[43] R. Gopal, J.S. Park, C.H. Seo, Y. Park, Applications of circular dichroism for structural analysis of gelatin and antimicrobial peptides, Int. J. Mol. Sci. 13 (2012) 3229–3244.
[44] Y.J. Na, S.B. Han, J.S. Kang, Y.D. Yoon, S.K. Park, H.M. Kim, K.H. Yang, C.O. Joe, Lactoferrin works as a new LPS-binding protein in inflammatory activation of macrophages, Int. Immunopharmacol. 4 (2004) 1187–1199.
[45] Y.J. Seo, K.T. Lee, J.R. Rho, J.H. Choi, Phorbaketal A, isolated from the marine sponge phorbas sp., exerts its anti-inflammatory effects via NF-kappaB inhibition and heme oxygenase-1 activation in lipopolysaccharide-stimulated macrophages, Mar. Drugs 13 (2015) 7005–7019.
[46] A. Gosslau, S. Li, C.T. Ho, K.Y. Chen, N.E. Rawson, The importance of natural product characterization in studies of their anti-inflammatory activity, Mol. Nutr. Food Res. 55 (2011) 74–82.
[47] C. Nathan, Points of control in inflammation, Nature 420 (2002) 846–852.
[48] A. van Dijk, M.H. Tersteeg-Zijderveld, J.L. Tjeerdsma-van Bokhoven, A.J. Jansman, E.J. Veldhuizen, H.P. Haagsman, Chicken heterophils are recruited to the site of Salmonella infection and release antibacterial mature Cathelicidin-2 upon stimulation with LPS, Mol. Immunol. 46 (2009) 1517–1526.
[49] M. Vaara, Agents that increase the permeability of the outer membrane, Microbiol. Rev. 56 (1992) 395–411.
[50] R.E. Hancock, Alterations in outer membrane permeability, Annu. Rev. Microbiol. 38 (1984) 237–264.
[51] A.H. Delcour, Outer membrane permeability and antibiotic resistance, Biochim. Biophys. Acta 1794 (2009) 808–816.
[52] D. Pletzer, S.R. Coleman, R.E.W. Hancock, Anti-biofilm peptides as a new weapon in antimicrobial warfare, Curr. Opin. Microbiol. 33 (2016) 35–40.
[53] X. Feng, K. Sambanthamoorthy, T. Palys, C. Paranavitana, The human antimicrobial peptide LL-37 and its fragments possess both antimicrobial and antibiofilm activities against multidrug-resistant Acinetobacter baumannii, Peptides 49 (2013) 131–137.
[54] D. Takahashi, S.K. Shukla, O. Prakash, G. Zhang, Structural determinants of host defense peptides for antimicrobial activity and target cell selectivity, Biochimie 92 (2010) 1236–1241.
[55] K.A. Brogden, Antimicrobial peptides: pore formers or metabolic inhibitors in bacteria? Nat. Rev. Microbiol. 3 (2005) 238–250.
[56] D.I. Chan, E.J. Prenner, H.J. Vogel, Tryptophan- and arginine-rich antimicrobial peptides: structures and mechanisms of action, Biochim. Biophys. Acta 1758 (2006) 1184–1202.
[57] M.L. Mangoni, A.M. McDermott, M. Zasloff, Antimicrobial peptides and wound healing: biological and therapeutic considerations, Exp. Dermatol. 25 (2016) 167–173.
[58] A. Tremel, A. Cai, N. Tirtaatmadja, B.D. Hughes, G.W. Stevens, K.A. Landman, A. J. O'Connor, Cell migration and proliferation during monolayer formation and wound healing, Chem. Eng. Sci. 64 (2009) 247.
[59] R.E.W. Hancock, K.L. Brown, N. Mookherjee, Host defence peptides from invertebrates—emerging antimicrobial strategies, Immunobiology 211 (2006) 315–322.
[60] R.E.W. Hancock, G. Diamond, The role of cationic anti-microbial peptides in innate host defences, Trends Microbiol. 8 (2000) 402–410.
[61] A.K. Marr, W.J. Gooderham, R.E.W. Hancock, Antibacterial peptides for therapeutic use: obstacles and realistic outlook, Curr. Opin. Pharmacol. 6 (2006) 468–472.
[62] E. Guaní-Guerra, T. Santos-Mendoza, S.O. Lugo-Reyes, L.M. Terán, Antimicrobial peptides: general overview and clinical implications in human health and disease, Clin. Immunol. 135 (2010) 1–11.
[63] P. Papareddy, M. Kalle, G. Kasetty, M. Mörgelin, V. Rydengård, B. Albiger, K. Lundqvist, M. Malmsten, A. Schmidtchen, C-terminal peptides of tissue factor pathway inhibitor are novel host defense molecules, J. Biol. Chem. 285 (2010) 28387–28398.
[64] E. Andersson, V. Rydengard, A. Sonesson, M. Morgelin, L. Bjorck, A. Schmidtchen, Antimicrobial activities of heparin-binding peptides, Eur. J. Biochem. 271 (2004) 1219–1226.
[65] S.G. Young, Recent progress in understanding apolipoprotein B, Circulation 82 (1990) 1574–1594.
[66] O.L. Franco, Peptide promiscuity: an evolutionary concept for plant defense, FEBS Lett. 585 (2011) 995–1000.
[67] H.M. Nguyen, C.J. Graber, Limitations of antibiotic options for invasive infections caused by methicillin-resistant *Staphylococcus aureus*: is combination therapy the answer? J. Antimicrob. Chemother. 65 (2010) 24–36.
[68] G.S. Tillotson, I. Dorrian, J. Blondeau, Fluoroquinolone resistance: mechanisms and epidemiology, J. Med. Microbiol. 46 (1997) 457–461.
[69] M.E. Evans, D.J. Feola, R.P. Rapp, Polymyxin B sulfate and colistin: old antibiotics for emerging multiresistant gram-negative bacteria, Ann. Pharmacother. 33 (1999) 960–967.
[70] H. Nakaido, M. Vaara, Molecular basis of bacterial outer membrane permeability, Microbiol. Rev. 49 (1985) 1–32.
[71] S.L. Percival, P. Kite, K. Eastwood, R. Murga, J. Carr, M.J. Arduino, Tetrasodium EDTA as a novel central venous catheter lock solution against biofilm, Infect. Control Hosp. Epidemiol. 2 (2005) 515–519.
[72] J. Overhage, A. Campisano, M. Bains, E.C. Torfs, B.H. Rehm, R.E.W. Hancock, Human host defense peptide LL-37 prevents bacterial biofilm formation, Infect. Immun. 76 (2008) 4176–4182.
[73] J.D. Heilborn, M.F. Nilsson, G. Kratz, G. Weber, O. Sørensen, N. Borregaard, M. Ståhle-Bäckdahl, The cathelicidin anti-microbial peptide LL 37 is involved in re epithelialization of human skin wounds and is lacking in chronic ulcer epithelium, J. Invest. Dermatol. 120 (2003) 379–389.
[74] R. Shaykhiev, C. Beisswenger, K. Kändler, J. Senske, A. Püchner, T. Damm, J. Behr, R. Bals, Human endogenous antibiotic LL-37 stimulates airway epithelial cell proliferation and wound closure, Am. J. Physiol. Lung Cell. Mol. Physiol. 289 (2005) L842–L848.